Investigating host-gut microbial relationship in Penaeus monodon upon exposure to Vibrio harveyi

Aquaculture

Angthong, Pacharaporn; Uengwetwanit, Tanaporn; Uawisetwathana, Umaporn; Koehorst, Jasper J.; Arayamethakorn, Sopacha et al

https://doi.org/10.1016/j.aquaculture.2023.739252

Aquaculture 567 (2023) 739252

Contents lists available at ScienceDirect

Aquaculture

journal homepage: www.elsevier.com/locate/aquaculture

Investigating host-gut microbial relationship in *Penaeus monodon* upon exposure to *Vibrio harveyi*

Pacharaporn Angthong [a], Tanaporn Uengwetwanit [a], Umaporn Uawisetwathana [a], Jasper J. Koehorst [b,c], Sopacha Arayamethakorn [a], Peter J. Schaap [b,c], Vitor Martins Dos Santos [g], Metavee Phromson [d], Nitsara Karoonuthaisiri [a,e,f], Sage Chaiyapechara [d], Wanilada Rungrassamee [a,*]

[a] *Microarray Research Team, National Center for Genetic Engineering and Biotechnology, National Science and Technology Development Agency, Pathum Thani 12120, Thailand*
[b] *Laboratory of Systems and Synthetic Biology, Department of Agrotechnology and Food Sciences, Wageningen University and Research, 6708WE Wageningen, The Netherlands*
[c] *UNLOCK, Wageningen University and Research, 6708WE Wageningen, The Netherlands*
[d] *Aquaculture Service Development Research Team, National Center for Genetic Engineering and Biotechnology, National Science and Technology Development Agency, Pathum Thani 12120, Thailand*
[e] *International Joint Research Center on Food Security, National Center for Genetic Engineering and Biotechnology, National Science and Technology Development Agency, Pathum Thani 12120, Thailand*
[f] *Institute for Global Food Security, Queen's University Belfast, Biological Sciences Building, 19 Chlorine Gardens, Belfast BT9 5DL, United Kingdom*
[g] *Laboratory of Bioprocess Engineering, Droevendaalsesteeg 1, 6708 PB Wageningen, The Netherlands*

ARTICLE INFO

Keywords:
Microbiome
Transcriptome
Metabolome
Pathogen exposure
Shrimp
Host-gut microbial relationship

ABSTRACT

To understand the host-gut microbial relationship, we used multidisciplinary platforms, metagenome, transcriptome, and metabolome analyses, to determine shrimp and intestinal microbial interactions upon 0, 6, 12, 24, and 48 h exposure to 10^7 CFU/mL of *Vibrio harveyi,* a shrimp pathogen. The bacterial communities in the intestine of shrimp were disrupted during exposure to *V. harveyi*. The abundance of *Vibrio* ASVs in the Harveyi and Vulnificus clades was significantly increased after exposure to the pathogen (6, 12, and 24 h) and decreased later after 48 h. Conversely, *Pseudoalteromonas* was found in lower abundance (6, 12, and 24 h) but significantly increased after 48 h of the bacterial challenge. Gene expression analysis revealed that genes belonging to several immune-related pathways, including the Toll pathway, the immune deficiency (IMD) pathway, and pattern recognition proteins (PRPs), were significantly upregulated. Early responses in the first 6 h after exposure were the genes involved in phagocytosis, pattern recognition proteins (PRPs), and signal transduction (*spätzle* and *ankyrin*). Late responses (12–48 h) were genes related to proteinases and proteinase inhibitors (PPIs), antimicrobial peptides (AMPs), and oxidative stress. Genes related to lipid metabolisms such as fatty acid metabolism and choline metabolism were also upregulated. Metabolomics analysis also showed an increase in phospholipids, including phosphocholine groups, in the intestine of shrimp exposed to the pathogen. Taken together, the gene expression and metabolomics analyses suggest the importance of lipid metabolism in the defense mechanism against bacterial invasion. Moreover, our metabolomic analysis showed a decrease in tryptophan and indole-3-acrylic acid, metabolites related to intestinal immune homeostasis, after bacterial infection. Our observations suggest that pathogenic *Vibrio* disrupted biological processes in the shrimp intestine, resulting in a decrease in indole-3-acrylic acid and its derivatives which in turn compromised intestinal immunity. In addition, shrimp responded to the bacterial invasion by activating metabolites related to eicosanoid and phospholipid biosynthesis. Our findings on the interactions between shrimp and intestinal microbiota will be an indispensable gateway to systems biology to better understand the function of shrimp gut microbiota and its influence on shrimp innate immunity.

* Corresponding author.
E-mail address: wanilada.run@biotec.or.th (W. Rungrassamee).

https://doi.org/10.1016/j.aquaculture.2023.739252
Received 28 August 2022; Received in revised form 11 December 2022; Accepted 8 January 2023
Available online 11 January 2023

1. Introduction

Shrimp aquaculture is an important industry that provides important source of seafood for the growing world's population. The black tiger shrimp (*Penaeus monodon*) is one of the major species cultivated in Southeast Asia and the coasts of Australia (FAO, 2016; Stentiford et al., 2012), with high market demand. However, shrimp production is facing major challenges, mainly due to the increase in disease outbreaks that are causing mass mortalities and inflicting severe economic losses on shrimp aquaculture (Kalaimani et al., 2013; Stentiford et al., 2012). The periodic outbreaks are caused by various pathogens such as viruses, bacteria, and fungi, with bacterial diseases being the main problem for shrimp aquaculture, mainly caused by *Vibrio* such as *V. harveyi*, *V. vulnificus* and *V. parahaemolyticus* (de Souza Valente and Wan, 2021; Flegel, 2019). Vibrios are ubiquitous in aquatic environments, including animal hosts (de Souza Valente and Wan, 2021; Rungrassamee et al., 2016), and some strains can become opportunistic pathogens under certain conditions (Zhang et al., 2021a). Vibrios can colonize the digestive system of shrimp by interacting with chitin molecules and producing chitinolytic enzymes and toxins that infect and destroy the digestive tract of shrimp, which can lead to mass mortality of shrimp in hatcheries and grow-out pond systems (Debnath et al., 2020; Montgomery and Kirchman, 1993; Soonthornchai et al., 2015). Among *Vibrio* species, *V. harveyi* has been reported to be the most virulent and widespread bacterial pathogen causing vibriosis, gastrointestinal diseases in shrimp aquaculture (Muthukrishnan et al., 2019; Zhang et al., 2020b). Therefore, disease control strategy for vibriosis is crucial for the sustainable production of shrimp aquaculture.

Intestinal bacteria play an important role in promoting host health by enhancing nutrient absorption, metabolic processes, physiological adaptation, immune response, and disease resistance in aquatic animals (Hanning and Diaz-Sanchez, 2015; Rajeev et al., 2020; Xiong et al., 2019). For instance, bacteria of the phylum Firmicutes can synthesize short-chain fatty acids and lactic acid-derived compounds, providing important metabolites for growth performance and health in many aquatic animals such as common carp (*Cyprinus carpio*) (Hoseinifar et al., 2015) and Atlantic salmon (*Salmo salar* L.) (Reveco et al., 2014). A previous study reported that *Brevibacillus*, which belongs to the phylum Firmicutes and has the ability to produce essential amino acid (Wang et al., 2015), was found in high abundance in the intestine of *P. monodon* and correlated with shrimp growth performance (Uengwetwanit et al., 2020). In addition, when given as feed additives, *Bacillus* sp. and *Lactobacillus* sp. have been reported to enhance shrimp resistance to *V. parahaemolyticus*, a causative pathogen of acute hepatopancreatic necrosis disease (AHPND) (Kewcharoen and Srisapoome, 2019) or *V. harveyi* in *Litopenaeus vannamei* (Kongnum and Hongpattarakere, 2012).

The intestine of shrimp contains a wide bacterial diversity that can be influenced by developmental stages, feed, and rearing environment (Angthong et al., 2020; Chaiyapechara et al., 2022; Holt et al., 2021). The most common bacteria in the intestine of shrimp are Proteobacteria, Bacteroidetes, Firmicutes, and Actinobacteria (Angthong et al., 2020; Rungrassamee et al., 2014; Wang et al., 2020). While commensal bacteria can colonize relatively stable in the gut, an invasion by pathogenic bacteria can disrupt host intestinal homeostasis (Davoodi and Foley, 2020; Rungrassamee et al., 2016; Wu et al., 2021). Changes in niche occupancy by intestinal bacteria may also contribute to the development of the disease (Pérez et al., 2010; Rajeev et al., 2020; Sehnal et al., 2021). Therefore, intestinal microbiota serves as a frontline interface to pathogens. Previous studies have shown that the bacterial communities in the intestine of healthy *L. vannamei* differ from those found in shrimp infected with diseases such as vibriosis, white feces syndrome, white spot syndrome, and AHPND (Alfiansah et al., 2020; Rungrassamee et al., 2016; Wang et al., 2019a; Yu et al., 2018).

As in other crustaceans, shrimp defense mechanisms depend entirely on the innate immune system, including cellular and humoral immune responses, to protect against invading microorganisms (Zhang et al., 2021c). Cellular immune responses consist of pattern recognition proteins (PRPs) on cell membranes that recognize and eliminate pathogens by phagocytosis, apoptosis, encapsulation, and nodulation (Jiravanichpaisal et al., 2006; Li and Xiang, 2013). On the other hand, humoral immune responses are activated by enzymes or factors in the hemolymph such as the prophenoloxidase (proPO) system, the blood coagulation system, lectins and antimicrobial peptides (AMPs) (Li and Xiang, 2013; Tassanakajon et al., 2018). The intestine is an important route of entry for pathogens to colonize and cause infection in crustaceans (Duan et al., 2018). Therefore, the shrimp intestine is constructed with a physical protective barrier of chitin and peritrophic matrix (PM) (Hegedus et al., 2009; Soonthornchai et al., 2015). However, if pathogens can breach these protective barriers and enter the host body, this can lead to the activation of host immune responses to maintain homeostasis (Bai et al., 2021; Silveira et al., 2018; Zhang and Sun, 2022). To control beneficial commensals and combat infectious pathogens, invertebrates must have an efficient microbial recognition system, signaling pathways, and effector molecules to combat invading pathogens (Kounatidis and Ligoxygakis, 2012). In the gut of pathogen-infected *Drosophila*, peritrophic matrix and epithelial integrity, production of reactive oxygen species (ROS), secretion of antimicrobial peptides (AMPs) into hemolymph are activated through immune deficiency (IMD) and Toll pathways, and epithelial renewal to maintain homeostasis in order to protect the gut damage (Kuraishi et al., 2013; Younes et al., 2020). In shrimp, the pathogen-infected intestine shows hemocyte infiltration into the intestinal epithelial cells (Silveira et al., 2018) and participates in the shrimp intestine by releasing immune molecules such as AMPs (i.e., *lysozyme*, *antilipopolysaccharide factor*, *crustin,* and *penaeidin*) (Silveira et al., 2018; Soonthornchai et al., 2010), PRPs (i.e., *C-type lectin*, *penlectin 5* and *mucin-like peritrophic membrane*) (Angthong et al., 2017; Soonthornchai et al., 2010), and *prophenoloxidase* (Soonthornchai et al., 2010) to protect against pathogen invasion. However, understanding of host-microbe interactions in the intestine of crustaceans including shrimp under pathogen exposure is still limited.

Recent advances in high-throughput omics platforms have provided important tools to better understand host-microbiota interactions (Wang et al., 2019b). For instance, the multi-omics approach of microbiome, transcriptome, and metabolome was applied to investigate the dynamics between host and gut microbiota under ammonia and heat stress in *L. vannamei*, leading to a better understanding of the association between host immune-related genes and gut bacteria under specific stress conditions (Duan et al., 2021). In addition, the multi-omics approach has led to identifying shrimp gut microbiota and host responses associated with *P. monodon* growth performance (Uengwetwanit et al., 2020). Here, we employed the multi-omic platform to explore the relationship between bacterial diversity and host responses in juvenile *P. monodon* following exposure to pathogenic *V. harveyi*. We were able to determine dynamics of intestinal bacterial composition, gene expression and metabolomic profiles in *P. monodon* intestine during the infection. Our findings provide a better understanding of possible molecular mechanisms of the shrimp host as well as the interaction between the host and the intestinal microbiota in response to the pathogen. Ultimately, this knowledge will lead to approaches to maintain gut microbial balance and application of gut microbial management in shrimp to improve the immune system in shrimp aquaculture.

2. Materials and methods

2.1. Ethics statement

All experimental protocols involving animals were approved by the Animal Ethics Committee at the National Center for Genetic Engineering and Biotechnology (approval code BT-Animal 04/2560) and conducted in accordance with relevant guidelines and regulations.

2.2. Shrimp and pathogen exposure trial

Black tiger shrimp, *Penaeus monodon* (approximately 3 g shrimp), were obtained from the Shrimp Genetic Improvement Center (Surat Thani, Thailand). Although certified SPF black tiger shrimp stock was not available at the time of the experiment, all shrimp used in this study were tested to be free of important pathogens affecting shrimp (Taura syndrome virus, white spot syndrome virus, yellow head virus, and infectious hypodermal and hematopoietic necrosis virus) using EZEE GENE PCR test kits (National Center of Genetic Engineering and Biotechnology, Thailand). Shrimp were acclimated in a tank containing seawater with a salinity of 20 ppt under the recirculation system (Fig. 1). After acclimation, 240 shrimp were randomly and equally distributed among cages (10 shrimp per cage). Shrimp were fed with commercial feed pellets (Inteqc, Thailand) at approximately 5% of body weight per day for five meals. Water quality was monitored every other day for temperature, pH, and dissolved oxygen and weekly for ammonia-nitrogen, nitrite-nitrogen, and alkalinity levels.

Vibrio harveyi AQVH001 was cultured in tryptic soy broth (TSB) medium plus 1.5% (*w/v*) NaCl and incubated for 18 h at 35 °C with shaking at 250 rpm. Bacterial cells were washed with 1.5% NaCl by centrifugation at 4500 rpm for 15 min at 4 °C. The cell pellet was resuspended in 1.5% NaCl and the bacterial concentration was estimated by using a spectrophotometer (Spectramax M5, Molecular Devices, USA) at OD 600 nm. The concentration of *V. harveyi* and the corresponding OD_{600nm} value were determined in advance and verified by a drop plate count method on thiosulfate-citrate-bile salts-sucrose (TCBS) agar plates (18 h at 35 °C).

For the immersion pathogen challenge, *V. harveyi* was added to the challenge tank at the final concentration of 10^7 CFUs/mL. Shrimp intestines ($n_{pooled} = 4$) were collected at 0, 6, 12, 24, and 48 h after the exposure for three replicates at each time point. Tissues were collected according to our previous work (Rungrassamee et al., 2014). Briefly, an intestine from each shrimp was aseptically dissected, and fecal matters were carefully and gently removed with sterile forceps before being placed in a sterile cryotube (Thermo Fisher Scientific, USA), then snap-frozen in liquid nitrogen and stored at −80 °C until use.

2.3. DNA extraction and purification

Each pooled intestine sample was ground in a mortar with liquid nitrogen. Each tissue sample (50 mg) was subjected to DNA extraction by using the QIAamp DNA Mini kit (Qiagen, Germany). DNA samples were purified and concentrated using the Genomic DNA Clean and Concentrator (Zymo Research, USA). DNA concentration and purity were quantified by using NanoDrop 8000 spectrophotometer (Thermo Fisher Science, USA), and stored at −20 °C.

2.4. 16S rRNA amplicon amplification and sequencing

The V3 and V4 regions were amplified with the following primer pairs; forward primer (5′ TCGTCGGCAGCGTCAGATGTGTATAAGAGACAGCCTACGGGNGGCWGCAG 3′) and reverse primer (5′

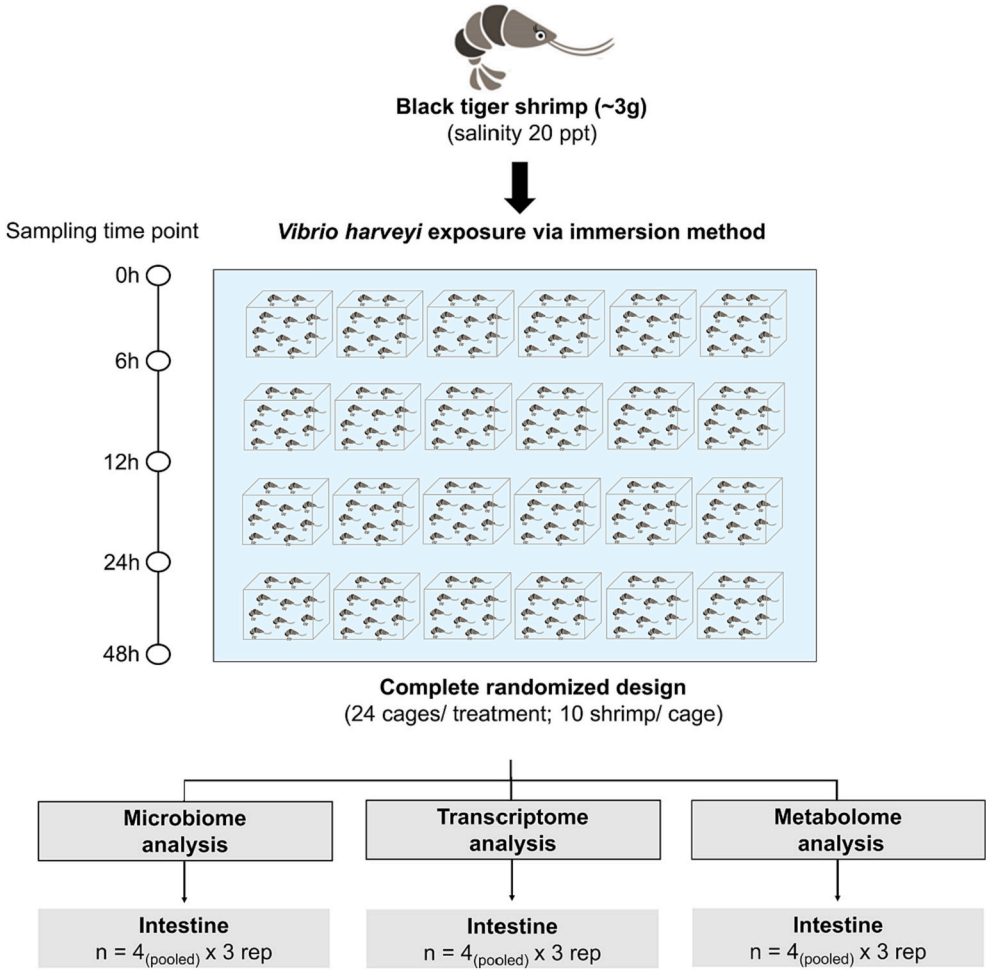

Fig. 1. Schematic representation of a time course *V. harveyi* exposure trial in the black tiger shrimp (*P. monodon*). Intestine samples were collected ($n_{pooled} = 4$ in triplicates) at 0, 6, 12, 24 and 48 h after the bacterial challenge for microbiome, transcriptome and metabolome analyses.

GTCTCGTGGGCTCGGAGATGTGTATAAGAGA-CAGGACTACHVGGGTATCTAATCC 3′). The 16S rRNA was amplified using a proofreading Q5 High-Fidelity DNA polymerase (New England Biolabs, USA) with the following program: 98 °C for 3 min, then 25 cycles of 98 °C for 30 s, 54 °C for 30 s and 72 °C for 30 s, and the final extension at 72 °C for 2 min. The PCR amplicons were visualized in 1.5% agarose gel electrophoresis and purified by using a QIAquick Gel Extraction Kit (Qiagen, Germany). The 16S rRNA amplicon libraries were sequenced by the Illumina MiSeq next-generation sequencing service (Macrogen Inc., Korea).

2.5. 16S rRNA amplicon data analysis

Primer sequences and low-quality bases of sequencing reads (250 × 2 bp, pair-end) were removed by using TrimGalore (Krueger et al., 2021). The reads longer than 200 bp, homopolymers < 6 bp, and the mean sequence quality score > 25 were further processed to remove chimeric sequences and generate an amplicon sequence variant (ASV) profile using DADA2 (Callahan et al., 2016) in Qiime2 (Bolyen et al., 2019). Taxonomic assignment was performed using BLAST+ consensus taxonomy classifier (Camacho et al., 2009) against the 16S SILVA database (version 132) (Quast et al., 2013). Results were exported and analyzed in R 4.0.3 (R Core Team, 2020; RStudio Team, 2020). Diversity analyses including Shannon diversity indices and principal coordinate analysis (PCoA) were performed using the Phyloseq package (McMurdie and Holmes, 2013). Total sum normalization was performed prior to comparative analysis between samples using Linear discriminant analysis effect size (LEfSe) (Segata et al., 2011). Differential abundant significant ASVs were determined based on the p-value <0.05 in the KruskalWallis test and Wilcoxon's test and a threshold logarithmic score of linear discriminant analysis (LDA) > 2.5. ASVs identified by LEfSe that belonged to *Vibrio* genus were further aligned with the *Vibrio* type strain data from the RDP database (http://rdp.cme.msu.edu/) and grouped into clades (Sawabe et al., 2013). A phylogenetic tree was constructed in MEGA X (Kumar et al., 2018) using the Maximum Likelihood method and Jukes-Cantor model (Jukes and Cantor, 1969). To derive the bacterial association pattern at each time point, the Pearson correlation-based ensemble approach of CoNet (Faust and Raes, 2016) was used. Prior to network construction, ASVs found in fewer than 3 replicates of at least one group were removed as they could cause artifactual associations (Faust and Raes, 2012). The Pearson correlation coefficient (r-value) was calculated between each pair of ASVs. These associations were represented as a network, where the nodes represent the ASVs of the bacteria and the edges represent the association between them. Permutation and Benjamin Hochberg were applied. Edge program with an r-value ≥0.9 (positive correlation) and an r-value ≥ −0.9 (negative correlation) and a p-value <0.05 were retained for the detection of microbial co-occurrence networks and visualized using Cytoscape (Shannon et al., 2003).

2.6. RNA extraction and RNAseq analysis

Each pooled intestine sample was ground to a fine powder using a pestle and mortar with liquid nitrogen. RNA was extracted using TRI Reagent (Molecular Research Center, USA) according to the manufacturer's protocol. All RNA samples were treated with 0.5 units/μg RQ1 RNase-free DNase (Promega, USA) to remove potential DNA contamination. The RNA concentration and purity were measured by NanoDrop (ND-8000) spectrophotometer, and its integrity was examined by 1% agarose gel electrophoresis. Each RNA library was prepared by using a TruSeq Stranded mRNA LT Sample Prep kit (Illumina, USA) according to the manufacturer's standard protocol. RNA sequencing analysis was performed using the Illumina Hiseq platform (Illumina, USA) (Macrogen Inc., Korea).

2.7. Transcriptomic data analysis

Sequencing reads were trimmed to remove adaptors and low-quality bases (Phread score <25) at both ends using TrimGalore (Krueger et al., 2021). After trimming, reads that were <100 bp were discarded. The quality of the reads was checked for each library using FastQC. Clean reads were mapped to the *P. monodon* genome (Uengwetwanit et al., 2021) using the default setting for splice-aware STAR (Dobin et al., 2012). Reads were quantified using featureCount (Liao et al., 2014). Deseq2 was used to normalize and quantify differential expression (Love et al., 2014). Prior to analysis, genes with low expression levels (count per million, CPM < 1 for >80% of the samples) were screened out. Genes with absolute fold-change values >1.0 and p-values <0.05 were considered as differentially expressed genes (DEGs). Gene functions were annotated using Blast2GO (Götz et al., 2008) with several databases including the NCBI non-redundant protein database, Eggnog (Huerta-Cepas et al., 2019), Gene Ontology (GO), and Reactome (Fabregat et al., 2016).

2.8. Validation of transcriptomic analysis by quantitative real-time PCR (qPCR) analysis

To validate the differential expression profiles from RNAseq analysis, eight genes of interest (*perlucin-like*, *C-type lectin 3*, *mannose-binding protein*, *spätzle 4-like isoform X3*, *lysozyme-like*, *astakine isoform X1*, *organic cation transporter protein-like isoform X2* and *mucin-5 AC-like isoform X1*) were selected for gene expression analysis by quantitative real-time PCR. Their immune-related function and $\log_2$ fold change values from RNAseq are shown in Table S1. Specific primer pairs for each gene were designed using Primer3 (Table S1). DNA-free RNA (1.5 μg) was reverse transcribed into cDNA using an ImPromII™ Reverse Transcriptase System kit (Promega, USA) according to the manufacturer's protocol. Each qPCR reaction contained 200 ng of cDNA, 0.2 μM of each primer and 1× SsoAdvanced Universal SYBR Green supermix (Bio-Rad, USA). Thermal cycling parameters were 95 °C for 30 s, followed by 40 cycles of 95 °C for 15 s, 56 °C for 30 s, 72 °C for 30 s and extension at 72 °C for 1 min. The melting curve analysis was performed from 65 °C to 95 °C in 0.5 °C increment steps with continuous fluorescent reading. The expression profile of each gene was calculated using the $2^{-\Delta\Delta CT}$ method (Livak and Schmittgen, 2001). Relative gene expression analysis was normalized to that the housekeeping gene (*elongation factor 1α*, *EF1α*) as an internal control. All qPCRs were performed in three biological replicates ($n = 3$). Results were statistically validated using one-way analysis of variance (ANOVA) followed by Duncan's new multiple range test in IBM SPSS statistics 23.0.

2.9. Metabolite extraction and profiling analysis

Shrimp intestines were collected ($n_{pooled} = 4$ in triplicates), and any visible fecal matters were removed. Then, frozen tissue samples were ground to fine powder using a ball mill grinder (MM400, Retsch). The shrimp sample was extracted using the previously published protocol (Uawisetwathana et al., 2021). Briefly, the shrimp intestine powder was dissolved in 1 mL of cold ethyl acetate:acetone (15:2 v/v) acidified with 0.5% acetic acid. The extraction process was performed twice, and the supernatant was collected and dried under vacuum using a TurboVap nitrogen evaporator (Biotage, Sweden). The dried samples were redissolved in acetonitrile (Optima LC/MS grade) and filtered through a micro centrifuge 0.22 μm PVDF membrane before transferring to an LC vial with a micro-insert for LC-HRMS-based metabolite profiling.

Untargeted metabolite profiles were analyzed by using Dionex RS3000 in coupled with a Thermo Scientific™ Orbitrap Fusion™ Tribrid™ mass spectrometer according to a previously published method (Uengwetwanit et al., 2020). Briefly, reverse-phase chromatography was performed with an HSS T3 C18 column (2.1 × 100 mm, 1.8 μm, Thermo) using a mobile phase (solvent A: water +0.1% acetic acid and

solvent B: acetronitrile +0.1% acetic acid) with a gradient elution system as follows: an isocratic period for 2 min at 99:1 (A:B), followed by a linear gradient to 1:99 (A:B) for 18 min, and a hold for 5 min, followed by restoring initial conditions 99:1 (A:B) for 1 min and hold for 5 min. Mass spectra were acquired using full scan data-dependent MS/MS in positive and negative electrospray ionization (ESI) modes over the mass range 50–1200 Da. The MS full scan resolution was set to 120,000 FWHM and the MS2 scan resolution was set to 15,000 FWHM with 25% higher-energy collisional dissociations (HCD). Pooled biological samples ($n_{pooled} = 20$) were used to measure reproducibility of the instrument. In addition, a "blank" sample (without shrimp intestine) was run in parallel as a control and used for subtraction in the data analysis.

2.10. Metabolite data processing and analyses

The acquired MS data from the samples, blanks and pooled samples were processed using Compound Discoverer (CD) 3.1.0 software with the following workflow: retention time alignment, unknown compound detection, elemental composition prediction, chemical background subtraction using blank samples and compound identification using ChemSpider, HMDB, KEGG, LipidMAPS (formula or exact mass), and mzCloud (mass fragmentation pattern). Processed metabolite features obtained in both positive and negative ESI modes were collected for analysis. The metabolite features affected by pathogen exposure were selected according to the following criteria: i) % coefficient of variation (CV) <60%, ii) fold change at their time 0 h. >1.5-fold, and iii) annotation confidence >80%. The patterns of change in the selected metabolite features were visualized in the form of a heat map.

2.11. Correlation analysis intestinal bacteria, DEGs and metabolites

Significant differentially abundant bacterial ASVs identified in this study from LEfSe analysis (LDA score > 2.6 and *p*-value <0.05), differentially expressed genes (absolute log2 fold-change values >1.0 and *p*-values <0.05) and differentially expressed metabolites (fold-change >1.5 and CV <60%) were used to determine the association between the multi-omic datasets. Log-ratio transformation using a geometric mean of the data at 0 h was used as a reference to determine the relative changes at each time point for calculating correlations. The relationship between bacterial ASVs and DEGs or metabolites was visualized in the early response (6 h) and late response (12 to 48 h) after the *V. harveyi* challenge. Spearman correlation was calculated and plotted using Himsc and Corrplot packages in R (Harrell and Dupont, 2019; Wei and Simko, 2021). Correlations were considered statistically significant if the |correlation coefficient| was >0.7.

3. Results

To understand the interaction of the intestinal bacteria with pathogen and the immune system, microbiome, transcriptome, and metabolome profiles were determined in intestine of *P. monodon* under a time-course exposure to *V. harveyi*, a shrimp pathogen (Fig. 1).

3.1. Comparison of intestinal bacterial profiles during pathogenic V. harveyi exposure

A total of 1,126,285 with an average (± standard deviation) of 75,086 ± 10,326 sequencing reads per sample and a range of 52,941 to 89,736 sequences were obtained after quality filtering (Table S2). A rarefaction curve based on the observed amplicon sequence variants (ASVs) reached a saturation plateau, indicating an overall sequencing depth adequately described the bacterial diversity in shrimp intestine samples (Fig. S1). The Shannon index, representing bacterial diversity, showed a significantly higher value in the shrimp intestine at 0 h (without *V. harveyi* exposure) than at 6 and 12 h after *V. harveyi* exposure (*p*-value <0.05) (Fig. 2A). Bacterial diversity decreased once shrimp were exposed to the pathogen and increased slightly again after 24 h, suggesting that the *V. harveyi* exposure disrupted the intestinal bacterial structure. Principal coordinate analysis (PCoA) performed based on the unweighted-UniFrac distance to compare the bacterial profiles associated in the intestine of shrimp during a time course exposure to *V. harveyi* showed the distinct separation of the bacterial communities from all time points after the exposure from the no exposure group (0 h) (Fig. 2B). These results indicated that the bacterial community shifted when shrimp were exposed to *V. harveyi*.

Relative bacterial abundance in *P. monodon* intestines was further determined and compared during the pathogen exposure (Fig. S2). At the phylum level, there were four major phyla present in all shrimp intestines, namely Proteobacteria, Bacteroidetes, Planctomycetes and Verrucomicrobia (Fig. S2A). Among these phyla, Proteobacteria was the most abundant. The top abundant genera from the four major phyla were compared at different time points of exposure to *V. harveyi* (Fig. S2B-E). Within phylum Proteobacteria, genus *Vibrio* was predominant at all time points of the pathogen exposure trial, however, the dominant bacterial genus shifted to *Pseudoalteromonas* at 48 h after pathogen exposure (Fig. S2B). Within phylum Bacteroidetes, *Tenacibaculum* was the most abundant genus in the intestine of the non-*V. harveyi* exposed shrimp, whereas the dominant bacterial genus shifted to *Mesoflavibacter* after the bacterial exposure (6, 24, 24 and 48 h) (Fig. S2C). *Carboxylicivirga* was found in relatively higher abundance in the shrimp at 0 and 6 h after pathogen exposure. The relative abundance of *Maribacter* and *Lewinella* increased at 6 and 12 h of the *V. haveyi* exposure, while the relative abundance of *NS3a* marine group increased at 12 h of *V. harveyi* exposure. In phylum Planctomycetes, *Planctomicrobium*, *Blastopirellula* and *Rhodopirellula* were the dominant genera in nearly all time points of the exposure (Fig. S2D). Unclassified *Rubinisphaeraceae* and *Gimesa* were also found associated in shrimp intestines in all treatment groups; however, these genera were present in higher abundant at 48 h after the *V. harveyi* challenge. The relative abundance of the *Pir4 lineage* was higher in the non-pathogen exposure group than in the *V. harveyi* challenged group. In addition, the genera *Haloferula* and *Roseibacillus* belonging to phylum Verrucomicrobia were found in high relative abundance in almost all time points of the *V. harveyi* challenge (Fig. S2E).

To determine the bacterial shifts in shrimp intestine after the exposure to *V. harveyi*, the significant bacterial changes of each exposure time point were compared using the linear analysis effect size (LEfSe) with linear discriminant analysis (LDA). The significant bacterial abundance found during the pathogen exposure belonged to phyla Verrucomicrobia, Proteobacteria, Planctomycetes, and Bacteroidetes (Fig. 3). *Haloferula*, *Aliiroseovarius*, *Defluviimonas*, *Roseovarius* and *Tenacibaculum* were significantly more abundant in the 0 h group. Different patterns of *Vibrio* diversity and dynamics were observed during the exposure period. The significant *Vibrio* ASVs were assigned to the closest matching type of *Vibrio* clades. This showed that the ASVs closely related to Orientalis were significantly found in the 0 h group. The ASVs belonging to the Harveyi clade were divided into two patterns, with five ASVs (ASV14474, ASV376, ASV11776, ASV8752, ASV968 and ASV14393) being more abundant in the 0 h group, and shifting to other ASVs (ASV11579, ASV7745, ASBV9460, ASV21, and ASV2957) in the 6 and 12 h groups. Similarly, ASVs belonging to the Vulnificus clade showed two patterns, with four ASVs (ASV8834, ASV9300, ASV12890 ASV9599) significantly found in the shrimp intestine at 0 h, and the others (ASV2459, ASV13095, ASV872, ASV12147, ASV240 and ASV9832) were more abundant at 6, 12 and 24 h. Interestingly, the abundance of *Vibrio* ASVs decreased at 48 h, while *Pseudoalteromonas* ASVs became relatively dominant.

3.2. Co-occurrence analysis of bacteria network in shrimp intestine during V. harveyi exposure

Co-occurrence network analysis was applied to examine the

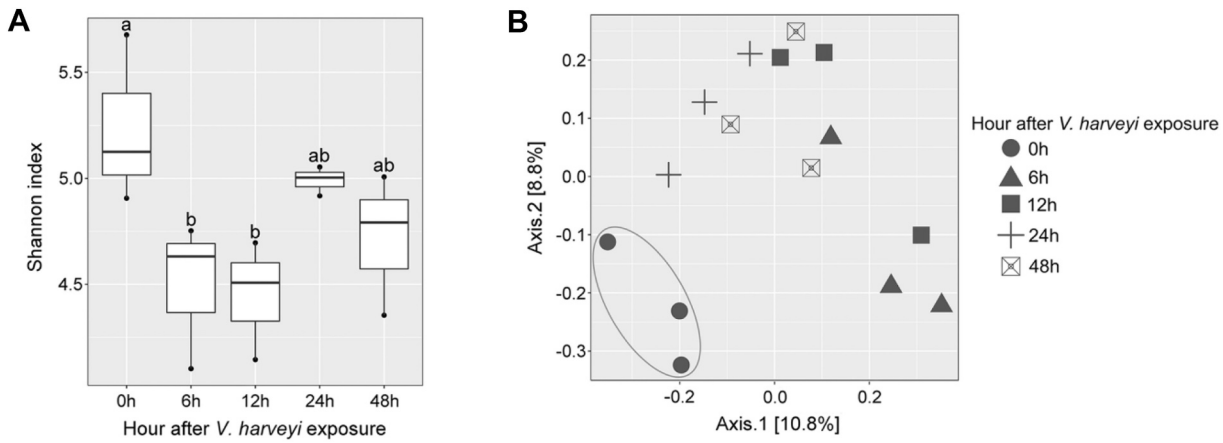

Fig. 2. Profiling of intestinal bacterial diversity analysis under the *V. harveyi* exposure. (A) Shannon index and (B) Principal Coordinate Analysis (PCoA) based on unweighted-UniFrac analysis of intestinal bacterial profiles of *P. monodon* after a time course exposure to *V. harveyi* at 0, 6, 12, 24 and 48 h. Different letters indicate significant differences between time points by ANOVA (p-value <0.05) ($n_{pooled} = 4$ in triplicates).

connections in the bacterial community found in shrimp intestine at each time point after the *V. harveyi* exposure (Fig. 4). The nodes represent statistically significant associations between bacterial taxa. The bacterial networks in the shrimp intestine at 0, 6, 12, 24 and 48 h exposure to the pathogen consisted of 127, 87, 85, 79 and 89 nodes, respectively (Fig. 4A). The unchallenged shrimp (0 h) had the most bacterial connections, which decreased later during the exposure (Fig. 4B-F). This trend was consistent with the bacterial diversity index (Shannon index) (Fig. 2A). Our results suggest that once pathogenic *V. harveyi* was present in the intestine of shrimp, bacterial diversity decreased along with reduced bacterial interactions. Our co-occurrence network analysis showed evidence of altered bacterial community structure in the presence of the pathogen (Fig. 4C-F) compared to a non-pathogen exposure group (Fig. 4B). For example, *Vibrio* ASVs were among the major central taxa that correlated with several bacterial groups, including Bacteroidetes, Planctomycetes, Firmicutes, and Proteobacteria (such as *Pseudoalteromonas* ASVs.). Interestingly, in the intestine of shrimp, *Vibrio* ASVs were found to be both positively and negatively correlated with *Pseudoalteromonas* ASVs at 12 h, in which the relationship became more negatively correlated at 24 h after the exposure (Fig. 4D and E).

3.3. Transcriptomic sequencing, assembly, and differentially expression analysis

To determine molecular mechanisms in shrimp during pathogenic bacteria exposure, transcriptomics analysis was carried in intestines of shrimp after the *V. harveyi* exposure at 0, 6, 12, 24 and 48 h with 3 replicates of each time point resulted in 42.5 ± 5.0 million reads on the average. After quality trimming, the reads were aligned to the *P. monodon* reference genome (Uengwetwanit et al., 2021). The sequencing reads obtained could be assigned to 91.2% of the genes in the reference genome, providing sufficient data to describe gene expression. Differentially expressed genes (DEGs) were measured by calculating log fold changes (FC) between groups 6, 12, 24 and 48 h and the group 0 h. The criteria for DEGs were positive $\log_2$ FC ≥ 1 or negative log2 FC ≥ −1 and p-value <0.05 (Fig. S3). Fold change was determined by using the 0 h group as a baseline compared with other time points of the pathogen exposure. A total of 783, 533, and 861 transcripts were differentially expressed at 6, 12, 24 and 48 h post pathogen exposure, respectively (Fig. S3A and Table S3). In addition, reactome pathway enrichment analyses were performed to determine the functional roles of these DEGs during the *V. harveyi* exposure in shrimp. Many pathways were mainly associated with metabolism, biological processes (i.e., signal transduction, post-translational protein modification, gene expression and RNA polymerase ii transcription) and the immune system, suggesting that they could play important roles in protection against pathogens (Fig. S3B).

3.4. Transcriptomic profiling in intestine of P. monodon during V. harveyi exposure

Gene expression profiles of *P. monodon* were determined over the time course of 6, 12, 24 and 48 h after pathogen challenge, comparing relative fold changes to an exposure time of 0 h (Fig. 5). As the primary defense mechanisms against pathogen invasion, the DEGs with their functions related to immune responses were further explored (Fig. 5A). The DEGs were classified into nine groups, which were pattern recognition proteins (PRPs), proteinases and proteinase inhibitors (PPIs), phagocytosis, signal transduction, antimicrobial peptides (AMPs), heat shock proteins (HSPs), oxidative stress responses, prophenoloxidase (proPO) system and other immune-related pathways. After 6 h of *V. harveyi* challenge, the up-regulated DEGs were mainly associated with PRPs (*perlucin-like*, *ficolin-1-like isoform X1* and *ficolin-2-like isoform X1*), phagocytosis (*low-density lipoprotein receptor 1-like* and *tubulin-specific chaperone cofactor E-like protein*), and signal transduction (*spätzle 4-like isoform X3*, *spätzle 5-like isoform X1*, *spätzle 5-like isoform X2,* and *ankyrin repeat and death domain-containing protein 1A-like*), suggesting that these immune-related genes were early responses with their roles as the first line of defense mechanisms. Although some of these immune-related genes showed decreasing expression levels at 12 h after the exposure, other immune-related genes were expressed in significantly high abundance in intestine at 24 and 48 h after the exposure. Several shrimp immune responses exhibiting a significant increase in expression after 12 to 48 h of the pathogen exposure were related to phagocytosis (*low-density lipoprotein receptor-like*, *low-density lipoprotein receptor-related protein 8-like* and *peroxisomal sarcosine oxidase-like*), AMPs (*lysozyme-like* and *i-type lysozyme-like protein 1*) and PPIs (*trypsin-like serine proteinase 2*, *trypsin-1-like, trypsinogen 1* and *trypsinogen 2*). In addition, PRPs (*mannose-binding protein* and *c-type lectins*), signal transduction (*spätzle 4-like isoform X3*, *spätzle 5-like isoform X1*and *spätzle 5-like isoform X2*), oxidative stress responses (*laccase 1* and *laccases-2-like*) and other immune-related genes (*astakine isoform X1* and *astakine isoform X2*) were significantly increased in the shrimp intestine at 24 and 48 h after the exposure. Some immune-related DEGs including *HSPs* and the *proPO* genes were down-regulated. Our gene expression profiling showed that shrimp elicited different immune gene responses over time during the exposure to *V. harveyi*.

In addition to the immune-related genes, significant DEGs involved in metabolic-related pathways were determined in the intestine of

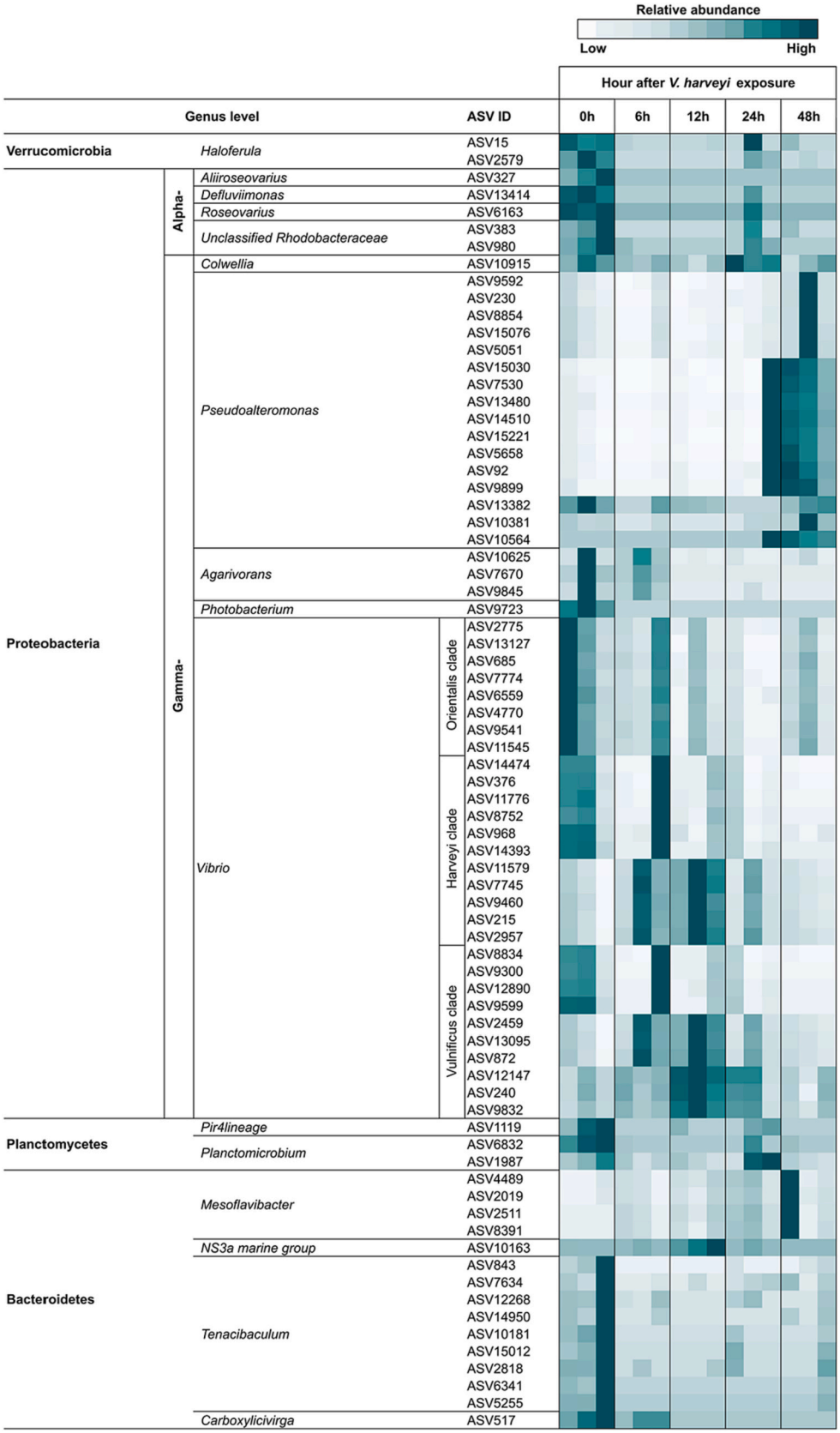

Fig. 3. LEfSe analysis showing the differential abundance of bacterial community in the intestines of *P. monodon* at 0, 6, 12, 24, and 48 h after exposure to the *V. harveyi*. The threshold value of the logarithmic linear discriminant analysis (LDA) score was 2.5 for *Vibrio* sp., and 2.0 for other bacterial species.

A

Co-occurrence networks	Hour after *V. harveyi* exposure				
	0h	6h	12h	24h	48h
Number of nodes	127	87	85	79	89
Average number of neighbors	51.94	24.46	29.84	23.95	28.18
Number of positive correlations	1760	753	616	645	859
Number of negative correlations	1538	311	652	301	395

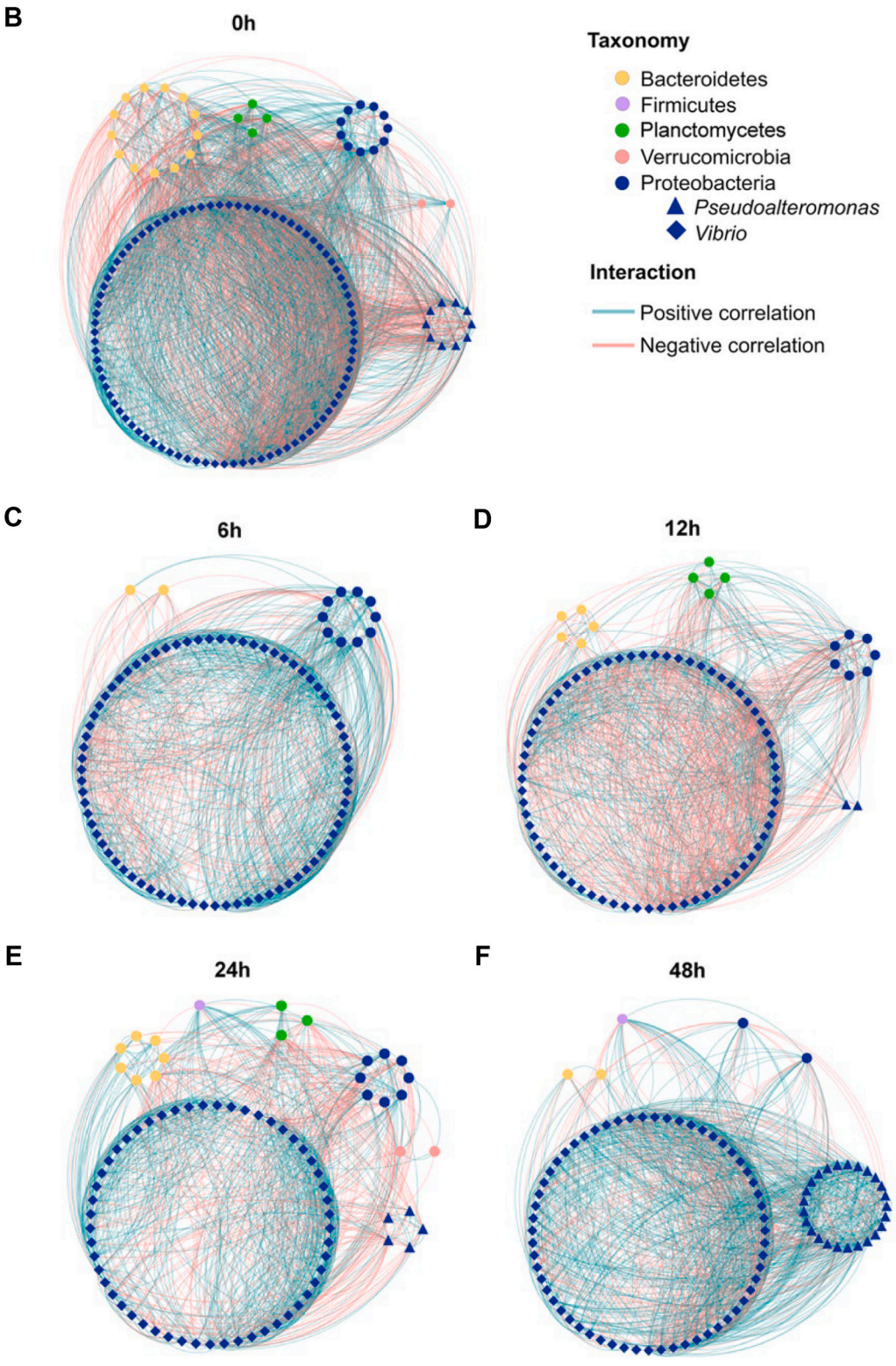

Fig. 4. Bacterial co-occurrence patterns in *P. monodon* intestines after an exposure to a pathogenic *V. harveyi*. (A) Number of significant ASVs in intestines of *P. monodon* during the exposure to *V. harveyi* at 0, 6, 12, 24 and 48 h. Microbial interaction network in shrimp intestine after the *V. harveyi* exposure at (B) 0, (C) 6, (D) 12, (E) 24 and (F) 48 h. The colour codes represent significant positive (blue) and negative (red) correlation in Pearson correlation (Pearson correlation coefficient, *r*-value $\geq$0.9 (blue) and ≥ -0.9 (red)). (For interpretation of the references to colour in this figure legend, the reader is referred to the web version of this article.)

A

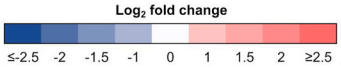

log2 fold change of DEGs				Immune-related genes
Hour after *V. harveyi* exposure				
6h	12h	24h	48h	
				Pattern recognition proteins
1.95	-1.21	0.56	0.84	*Perlucin-like*
1.47	0.39	1.72	0.28	*Ficolin-2-like isoform X1*
1.45	0.33	1.67	0.26	*Ficolin-1-like isoform X1*
0.42	0.75	1.01	0.89	*C-type lectin 2*
-0.02	-0.15	0.72	1.25	*C-type lectin domain family 4 member E-like*
-0.07	-0.13	0.72	1.27	*C-type lectin 3*
0.24	0.13	1.55	1.67	*Mannose-binding protein*
-0.52	0.17	-0.14	-1.07	*C-type mannose receptor 2-like isoform X2*
0.58	0.19	0.46	-1.29	*Ladderlectin-like isoform X2*
-0.79	-0.93	-1.22	-2.02	*Ladderlectin-like*
				Signal transduction
2.39	-0.30	2.69	2.23	*Spätzle 4-like isoform X3*
2.41	0.06	2.82	2.29	*Spätzle 5-like isoform X1*
2.52	0.10	2.96	2.54	*Spätzle 5-like isoform X2*
1.06	0.46	0.21	0.32	*Ankyrin repeat and death domain-containing protein 1A-like*
0.35	1.09	0.55	0.59	*Ankyrin-3-like*
-1.08	-0.20	-0.58	-0.64	*Ankyrin-1-like*
-1.15	0.39	-1.43	-0.43	*Toll-like receptor 3*
				Phagocytosis
-0.31	2.75	4.41	5.00	*Low-density lipoprotein receptor-like*
-0.31	2.75	4.41	5.00	*Low-density lipoprotein receptor-related protein 8-like*
0.74	2.18	1.30	1.32	*Peroxisomal sarcosine oxidase-like*
1.06	0.79	0.95	0.59	*Low-density lipoprotein receptor 1-like*
1.03	0.72	0.56	0.07	*Tubulin-specific chaperone cofactor E-like protein*
-0.55	-0.52	-1.09	-0.64	*Tubulin alpha-8 chain-like*
-1.29	0.22	-1.25	-1.00	*Tubulin alpha-1 chain*
-1.85	-1.39	-0.22	-0.77	*Kinesin-like protein KIF21B*
				Antimicrobial peptides
-1.07	2.49	4.73	3.14	*Lysozyme-like*
-1.07	2.49	4.73	3.14	*i-type lysozyme-like protein 1*
-0.19	0.16	-0.18	-1.27	*Lysozyme C-like*
-0.49	-0.20	-1.17	-0.54	*Penaeidin-2b-like*
-1.15	-0.21	-1.38	-0.97	*Penaeidin-4c-like*
-0.78	-0.44	-1.58	-0.85	*Crustin Pm4 antimicrobial peptide*
-0.69	-0.46	-1.61	-0.83	*Putative antimicrobial peptide*
-1.14	-0.47	-1.65	-0.97	*Penaeidin-3*
				Proteinases and proteinase inhibitors
0.56	1.55	0.81	0.55	*Caspase-1-like isoform X2*
-1.32	1.36	4.59	3.46	*Trypsin-like serine proteinase 2*
-1.32	1.36	4.59	3.46	*Trypsin-1-like*
-1.32	1.37	4.59	3.46	*Trypsinogen 1*
-1.32	0.95	4.44	3.43	*Trypsinogen 2*
-1.33	-0.81	-0.86	-1.18	*Caspase-2-like isoform X2*
-1.34	-0.81	-0.89	-1.20	*Caspase-2-like isoform X3*
-1.03	0.58	-1.47	-0.59	*CLIP domain-containing serine protease 2-like*
-0.65	0.09	-1.11	-1.51	*Kazal-type protease inhibitor*
-0.97	0.44	-1.37	-0.50	*Protease-like isoform X2*
-0.38	-2.26	-0.93	-5.43	*Trypsin 3A1-like*
-1.22	-0.84	-0.92	-1.63	*Trypsin-2-like*
				Heat shock proteins
0.46	1.28	0.92	0.57	*Heat shock 70 kDa protein 12A-like*
-1.03	-0.35	-0.07	0.56	*Heat shock protein HSP 90-alpha-like*
-1.03	-0.35	-0.07	0.56	*Heat shock protein 90*
-1.81	-1.55	-1.64	0.95	*Heat shock protein 22-like*
-1.56	-1.26	-0.64	0.16	*Heat shock protein 21*
-1.76	-1.91	-1.68	0.06	*Heat shock protein 22-like isoform X2*
-1.87	-1.87	-1.75	-0.09	*Heat shock protein 22-like isoform X1*
-0.99	-0.82	-1.05	-0.98	*Heat shock protein beta-1-like*
				Oxidative stress responses
0.63	0.70	1.64	1.09	*Laccase 1*
0.60	0.65	1.59	1.05	*Laccase-2-like*
-1.04	-1.08	-1.43	-1.27	*Probable glutathione peroxidase 8*
-1.04	-1.08	-1.43	-1.27	*Glutathione peroxidase 7-like*
-1.61	0.52	-2.11	-1.17	*NADPH oxidase 5-like*
				Prophenoloxidase system
-0.33	-0.42	-1.19	-1.49	*Phenoloxidase-activating factor 1-like isoform X2*
-0.57	-0.59	-0.87	-1.25	*Phenoloxidase-activating factor 2-like isoform X1*
-0.68	-0.61	-0.88	-1.32	*Phenoloxidase-activating factor 2-like isoform X2*
-1.45	-1.37	-1.39	-2.73	*Peroxidase-like*
-0.64	-0.40	-0.78	-1.54	*Melanization interacting protein*
-1.07	-0.28	-1.32	-1.24	*Prophenoloxidase activating factors*
				Other immune-related pathways
1.06	-0.02	1.67	2.34	*Astakine isoform X1*
1.06	-0.02	1.67	2.34	*Astakine isoform X2*
-1.43	-0.50	-1.45	-2.33	*Thrombospondin type-1 domain-containing protein 7B-like*
-0.73	0.78	-1.47	-1.66	*Matrix metalloproteinase-14-like*
-1.00	0.76	-1.30	-0.44	*Matrix metalloproteinase-14-like isoform X2*
-1.00	0.76	-1.30	-0.44	*Matrix metalloproteinase-14-like isoform X1*
-1.17	-1.10	-0.18	-0.32	*Suppressor of cytokine signaling-2 like protein*

Fig. 5. Heatmap depicting the differentially expressed genes (DEGs) enriched in (A) immune-related pathways and (B) energy- and metabolic-related pathways in *P. monodon* intestines during the *V. harveyi* exposure. Transcripts were considered differentially expressed when they had at least $\log_2$ fold change >1 with count per million >1 in all replicates ($n = 3$). Fold change was determined by using the 0 h group as a baseline and comparing to the 6, 12, 24 and 48 h exposure period groups.

B

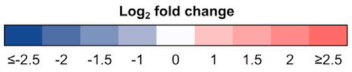

log2 fold change of DEGs Hour after *V. harveyi* exposure 6h	12h	24h	48h	Energy and metabolic-related genes
				Fatty acid metabolism
3.32	2.46	1.55	1.48	*Fatty acid binding protein 1-B.1-like*
1.40	1.45	0.35	0.78	*4-coumarate--CoA ligase 1*
1.39	1.44	0.34	0.77	*4-coumarate--CoA ligase 1-like isoform X1*
1.09	0.74	0.23	0.45	*Peroxisome proliferator-activated receptor alpha-like*
0.49	0.81	1.00	0.82	*Acetyl-CoA carboxylase-like isoform X1*
0.17	0.69	2.38	1.91	*Fatty acid synthase-like*
-0.58	-1.10	0.39	0.13	*Polyunsaturated fatty acid 5-lipoxygenase-like isoform X2*
				Choline metabolism
1.46	1.66	1.35	0.39	*Organic cation transporter protein-like isoform X1*
1.56	1.73	1.42	0.41	*Organic cation transporter protein-like isoform X2*
1.56	1.73	1.42	0.41	*Organic cation transporter protein-like isoform X3*
0.21	1.04	0.28	0.03	*Solute carrier family 22 member 20-like*
				Purine/Pyrimidine metabolism
1.07	0.75	0.96	0.68	*Dihydropyrimidine dehydrogenase [NADP(+)]-like*
1.05	0.59	0.75	0.49	*High affinity cAMP-specific and IBMX-insensitive 3',2C5'-cyclic phosphodiesterase 8*
0.82	1.17	0.92	0.48	*Phosphodiesterase 2-like*
0.52	1.01	0.74	-0.44	*Head-specific guanylate cyclase-like*
0.43	-0.14	2.30	-0.98	*Adenylate kinase isoenzyme 1-like*
-0.70	-0.07	-0.63	-1.20	*Xanthine dehydrogenase/oxidase-like*
-0.93	-1.25	-1.34	-1.04	*Deoxynucleoside triphosphate triphosphohydrolase SAMHD1-like*
-1.54	-1.11	-0.86	-2.41	*Peptidylglycine alpha-hydroxylating monooxygenase-like isoform X4*
				Gluconeogenesis
0.89	1.17	1.08	1.31	*Aldo-keto reductase family 1 member A1-like*
-0.79	-0.01	-1.25	-0.90	*Triosephosphate isomerase*
-1.66	-1.30	-0.24	-0.54	*Phosphoenolpyruvate carboxykinase,2C cytosolic [GTP]-like isoform X1*
-1.63	-1.29	-0.24	-0.54	*Phosphoenolpyruvate carboxykinase,2C cytosolic [GTP]-like isoform X2*
-1.97	-1.54	0.46	-1.64	*Triosephosphate isomerase-like*
				Glycerophospholipid metabolism
0.49	0.26	0.52	1.35	*Cholinesterase 2-like*
0.63	1.26	0.92	0.56	*Phospholipase D alpha 1-like*
-0.62	0.57	-1.33	-0.81	*5'-3' exonuclease PLD3-like isoform X1*
-0.62	0.69	-1.26	-0.74	*5'-3' exonuclease PLD3-like isoform X2*
-0.62	0.57	-1.33	-0.80	*5'-3' exonuclease PLD3-like isoform X3*
-1.21	-0.70	-0.89	-0.94	*Glycerol-3-phosphate dehydrogenase, mitochondrial-like isoform X2*
-1.21	-0.40	-1.40	-0.99	*Glycerophosphocholine cholinephosphodiesterase ENPP6-like*
-1.86	0.28	-1.99	-1.57	*Diacylglycerol kinase theta-like isoform X2*
0.62	0.21	-1.21	-2.02	*Glycerol-3-phosphate acyltransferase 3-like*
-0.78	-0.05	-1.24	-2.42	*Lysocardiolipin acyltransferase 1-like*
				Amino sugar and nucleotide sugar metabolism
0.84	1.10	1.34	0.65	*Beta-hexosaminidase subunit beta-like*
-0.30	0.27	-1.14	-0.27	*Acidic mammalian chitinase-like isoform X1*
-0.27	0.30	-1.13	-0.26	*Acidic mammalian chitinase-like isoform X2*
-4.40	-2.63	-2.20	-7.82	*Probable chitinase 10*
-4.40	-2.53	-2.15	-7.55	*Chitinase 2*
				Aminoacyl-tRNA biosynthesis
-1.07	-0.80	-0.39	-0.61	*Phenylalanine--tRNA ligase alpha subunit-like*
-1.20	-0.83	-0.34	-0.52	*Tyrosine--tRNA ligase, cytoplasmic-like isoform X1*
-1.20	-0.83	-0.35	-0.53	*Tyrosine--tRNA ligase,2C cytoplasmic-like isoform X1*
-1.20	-0.83	-0.35	-0.52	*Tyrosine--tRNA ligase,2C cytoplasmic-like isoform X2*
-1.17	-0.87	-0.42	-0.70	*Valine--tRNA ligase-like isoform X1*
-1.17	-0.88	-0.42	-0.68	*Valine--tRNA ligase-like isoform X2*
				Chitin metabolism
7.27	2.54	7.62	7.22	*Chitin binding domain*
5.69	2.52	4.14	3.34	*Cuticle protein 2-like*
5.01	2.53	3.86	3.04	*Cuticle protein AM1159-like*
3.95	2.21	4.43	3.90	*Mucin-5AC-like isoform X1*
-3.20	-2.90	-2.82	-1.09	*Endochitinase A1-like*
-2.13	-2.93	-1.81	-1.10	*Peritrophin-55-like*

Fig. 5. (*continued*).

shrimp during the *V. harveyi* challenge (Fig. 5B). The genes involved in fatty acid metabolism (*fatty acid binding protein 1-B.1-like*, *4-coumarate-CoA ligase 1*, *4-coumarate-CoA ligase 1-like isoform X1*, *peroxisome proliferator-activated receptor alpha-like*, *acetyl-CoA carboxylase-like isoform X1* and *fatty acid synthase-like*) and choline metabolism (*organic cation transporter proteins-like* and *solute carrier family 22 member 20-like*) were up-regulated throughout the period of bacterial challenge. DEGs related to chitin metabolism (*chitin binding domain*, *cuticle protein 2-like*, *cuticle protein AM1159-like* and *mucin-5AC-like isoform X1*) exhibited significantly high expression levels in the shrimp intestine during the challenge. Metabolic genes involved in purine/pyrimidine metabolism (*dihydropyrimidine dehydrogenase [NADP(+)]-like*, *high affinity cAMP-specific and IBMX-insensitive 3',2C5'-cyclic phosphodiesterase 8* and *phosphodiesterase 2-like*), gluconeogenesis (*aldo-keto reductase family 1 member A1-like*) and glycerophospholipid metabolism (*cholinesterase 2-like* and *Phospholipase D alpha 1-like*) were up-regulated, whereas genes involved in aminoacyl-tRNA biosynthesis were down-regulated during the *V. harveyi* exposure such as *phenylalanine-tRNA ligase alpha subunit-like*, *tyrosine-tRNA ligase, cytoplasmic-like isoform X1* and *valine-tRNA ligase-like isoform X1*.

To validate the gene expression profile obtained from RNAseq analysis, real-time PCR was performed to determine the transcript levels of the eight selected genes (*perlucin-like*, *c-type lectin 3*, *mannose-binding protein*, *spätzle 4-like isoform X3*, *lysozyme-like*, *astakine isoform X1*, *organic cation transporter protein-like isoform X2* and *mucin-5 AC-like isoform X1*). The candidate genes were selected based on their immune-related function and $\log_2$ fold change patterns from RNAseq analysis (Table S1). The expression patterns of all genes determined by real-time PCR were consistent with the gene expression patterns from RNAseq (Fig. S4).

A

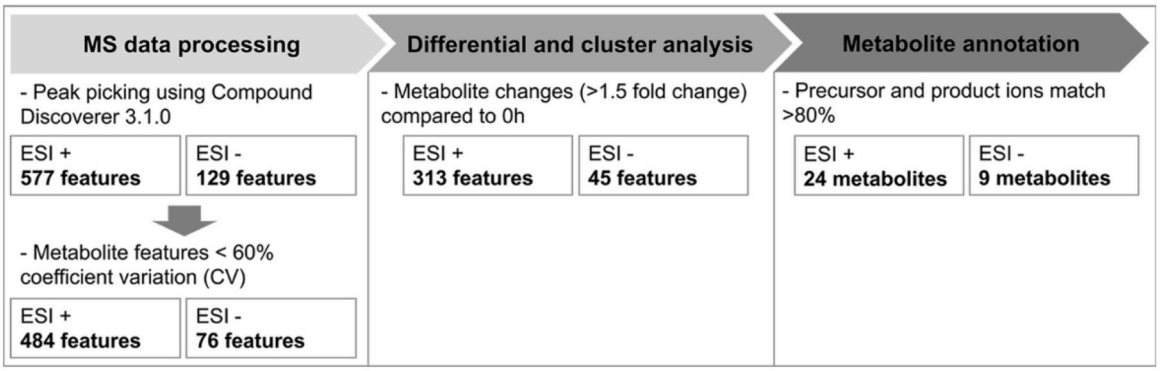

B

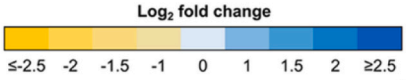

log2 fold change of metabolites				Metabolites
Hour after *V. harveyi* exposure				
6h	12h	24h	48h	
				Prenol lipids
1.13	-2.72	0.97	-1.06	L-menthyl acetoacetate
				Fatty acids
0.87	-0.90	2.44	0.23	α-linolenic acid
1.66	-1.31	3.08	0.91	13-hydroxy-9E,11E-octadecadienoic acid (13-HODE)
0.47	0.35	1.24	0.94	8-hydroxyeicosapentaenoic acid (8-HEPE)
1.05	0.59	0.92	0.21	10-oxo-8-decenoic acid
-0.24	-1.04	1.28	-1.58	7-(2-Cyclopenten-1-yl)heptanoic acid
-1.43	-2.48	1.37	-1.33	13-oxotrideca-9,11-dienoic acid
				Phospholipids
-0.93	-1.11	3.08	0.73	1-(9Z-hexadecenoyl)-sn-glycero-3-phosphoethanolamine (LPE(16:1))
-0.69	-1.62	0.85	1.41	1-[(9Z)-hexadecenoyl]-sn-glycero-3-phosphocholine (LPC(16:1/0:0))
-0.60	-1.35	1.00	1.75	L-α-lysophosphatidylcholine (L-α-LPC)
-0.16	-1.00	0.82	1.36	LysoPC(20:5(5Z,8Z,11Z,14Z,17Z)) (LPC(20:5n3/0:0))
-0.36	-1.28	1.14	1.38	2-oleoyl-sn-glycero-3-phosphocholine (LPC(0:0/18:1))
0.16	-1.53	1.13	2.29	1-(4Z,7Z,10Z,13Z,16Z,19Z-docosahexaenoyl)-sn-glycero-3-phosphocholine (LPC(22:6w3/0:0))
-0.33	-0.75	1.03	1.79	2-palmitoyl-sn-glycero-3-phosphocholine (LPC(0:0/16:0))
-1.35	0.35	0.58	0.68	Glycerophospho-N-palmitoyl ethanolamine (GP-NPEA)
				Fatty-amino acids conjugate
-0.98	1.43	0.98	1.00	Cervonyl carnitine
-0.27	0.21	0.91	1.17	N-Stearoyltyrosine
0.54	1.19	0.99	0.91	Palmitoylcarnitine
				Purines/pyrimidines and derivatives
0.08	-1.27	-0.59	-1.11	Uridine
-0.40	-2.84	-1.74	-2.18	Guanosine
-2.18	-2.59	-1.48	-1.45	Thymine
-0.94	-2.05	-0.72	-0.88	Inosine
-1.53	-3.03	-0.55	-1.46	2'-Deoxyadenosine
-1.86	-2.20	-0.90	-1.83	Thymidine
-1.21	-1.25	-0.69	-0.34	Xanthopterin
-0.78	-0.52	0.05	-0.91	Uric acid
				Peptides
-1.08	-0.45	-0.36	-0.83	Trp-Phe
-1.01	-1.62	-1.91	0.10	Leu-Asp
-1.27	-1.30	-0.35	-1.18	Trp-Ile
-0.14	-2.09	-1.74	0.87	Formylmethionyl-leucyl-phenylalanine methyl ester (For-Met-Leu-Phe-Ome)
				Amino acids and derivatives
-0.48	-1.09	-0.46	-0.90	Tryptophan
-0.48	-1.09	-0.46	-0.91	Indole-3-acrylic acid
				Pyridines and derivatives
-1.93	-2.68	-1.26	-1.52	Nicotinamide

Fig. 6. Analysis of metabolite profiles in *P. monodon* intestines under the *V. harveyi* exposure. (A) Workflow of untargeted metabolomics analysis, (B) heatmap showing the significant metabolites in *P. monodon* intestines affected by *Vibrio* at 6, 12, 24 and 48 h, and (C) The proposed model of metabolites and metabolic pathways in *P. monodon* intestine upon the *V. harveyi* exposure. Blue box represents energy- and metabolic-related genes, while pink box represents metabolites in *P. monodon* intestines during the *V. harveyi* exposure. (For interpretation of the references to colour in this figure legend, the reader is referred to the web version of this article.)

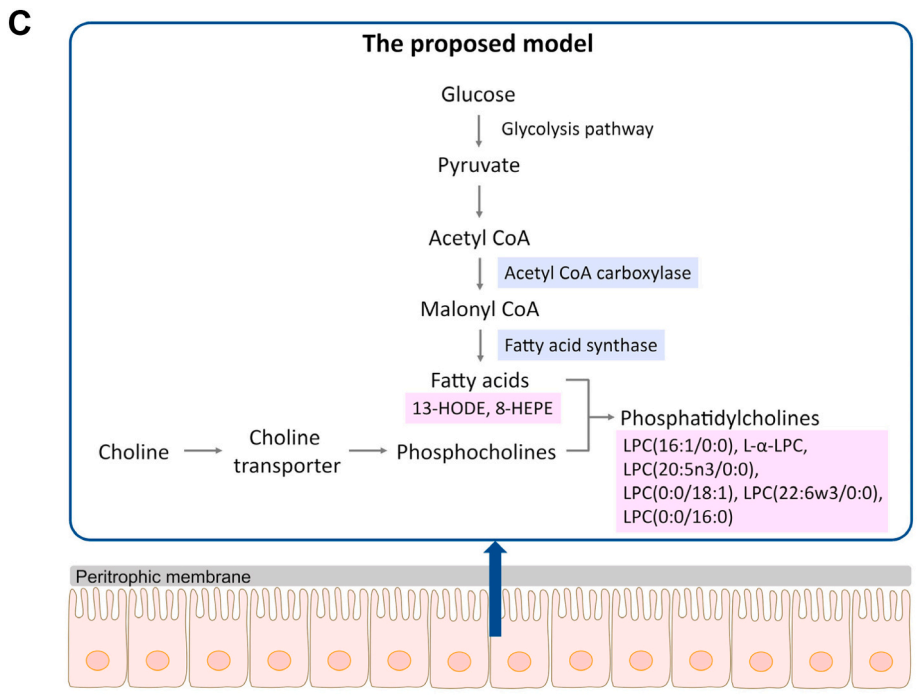

Fig. 6. (*continued*).

3.5. Metabolomics profiles in shrimp intestines under Vibrio challenge

The untargeted metabolomics data were determined to understand the changes in the physiological state of the host upon exposure to the pathogen (Fig. 6). The MS processed data of the shrimp intestines under the *Vibrio* challenge revealed 577 ions for the ESI+ mode and 129 ions for the ESI- mode (Fig. 6A). These metabolite features were then filtered for inter-replicate reproducibility by selecting metabolites with % coefficient of variation (%CV) < 60% (484 for ESI+ and 76 for ESI-), and > 1.5-fold when compared to the 0 h group (313 for ESI+ and 45 for ESI-). Then, the annotated metabolites with >80% confidence level were selected for biological interpretation (24 for ESI+ and 9 for ESI-).

The relative changes in metabolites at 6, 12, 24 and 48 h after the *Vibrio* exposure were compared to the 0 h group (Fig. 6B). The observed metabolites could clearly be classified into two patterns of increasing and decreasing metabolite concentrations during the pathogen exposure. At 24 and 48 h after bacterial challenge, the significantly increased metabolites include fatty acids (e.g. α-linolenic acid, 13-hydroxy-9E,11E-octadecadienoic acid (13-HODE) and 8-hydroxyeicosapentaenoic acid (8-HEPE)) and phospholipids (e.g. 1-(9Z-hexadecenoyl)-sn-glycero-3-phosphoethanolamine (LPE(16:1)), 1-[(9Z)-hexadecenoyl]-sn-glycero-3-phosphocholine (LPC(16:1/0:0)), L-α-lysophosphatidylcholine (L-α-LPC), 2-oleoyl-sn-glycero-3-phosphocholine (LPC(0:0/18:1)) and 2-palmitoyl-sn-glycero-3-phosphocholine (LPC(0:0/16:0))). Moreover, fatty-amino acid conjugates (cervonyl carnitine, N-stearoyltyrosine and palmitoylcarnitine) were found in slightly elevated concentrations between 12 and 48 h of the exposure. On the other hand, metabolites with decreased concentrations after the *V. harveyi* exposure include purines/pyrimidines and derivatives (e.g., uridine, guanosine, thymine and inosine), peptides (Trp-Phe, Leu-Asp, Trp-Ile and formylmethionyl-leucyl-phenylalanine methyl ester (For-Met-Leu-Phe-Ome)), amino acids and derivatives (tryptophan and indole-3-acrylic acid) and pyridine and derivative (nicotinamide). Additionally, fatty acids (13-HODE and 8-HEPE) and phosphatidylcholine (LPC(16:1/0:0), L-α-LPC, LPC(20:5n3/0:0), LPC(0:0/18:1), LPC(22:6w3/0:0) and LPC (0:0/16:0)) in glycolysis, which were correlated with the DEGs of *acetyl-CoA carboxylase* and *fatty acid synthase*, can also be synthesized via the choline metabolism pathway (Fig. 6C).

3.6. Correlation analysis among intestinal microbiota, differentially expressed genes and metabolites

To determine the interaction between intestinal microbiota, shrimp immune responses and metabolites at the early (6 h) and later time points (12 to 48 h) of exposure to *V. harveyi*, correlation analyses were performed between bacterial ASVs, DEGs related to immune responses and metabolites using Spearman correlation analysis (Fig. 7 and Table S4). At the onset of pathogen exposure, intestinal bacterial genera such as *Haloferula*, *Pseudoalteromonas*, *Tenacibaculum* and *Vibrio* mostly showed negative correlation with immune-related DEGs involved in PPRs, phagocytosis, PPIs, oxidative stress responses, and AMPs. *Vibrio* ASVs were positively correlated with DEGs involved in PRPs, phagocytosis and PPIs at the late stage of bacterial exposure (12 to 48 h), whereas *Pseudoalteromonas* ASVs were negatively correlated with DEGs involved in PRPs. When correlating intestinal bacteria with metabolites, the *Vibrio* ASVs were negatively correlated with metabolites related to fatty acids, phospholipids and amino acids and derivatives at the beginning (6 h) and later stages (12 to 48 h) of exposure to *V. harveyi* (Fig. 7 and Table S4). Interestingly, *Pseudoalteromonas* ASVs were negatively correlated with fatty acids, phospholipids and amino acids and derivatives at the beginning of bacterial exposure but showed the opposite pattern of this metabolite correlation.

4. Discussion

Vibriosis is one of the most important shrimp diseases affecting shrimp production (de Souza Valente and Wan, 2021; Zhang et al., 2020b). The disease is caused by opportunistic vibrios such as *V. harveyi*, and the pathogen can disrupt intestinal microbiota diversities and host homeostasis (Rungrassamee et al., 2016). Therefore, understanding bacterial dynamics and host defense mechanisms during *V. harveyi* exposure is important for managing disease control in shrimp aquaculture. Here, we used multi-omics analyses to determine the correlation among the intestinal microbiota, host gene expression and metabolites of *P. monodon* upon an exposure to the pathogenic *V. harveyi*.

In this study, the shift of the bacterial community structures in shrimp intestines during the exposure to *V. harveyi* was observed. Our

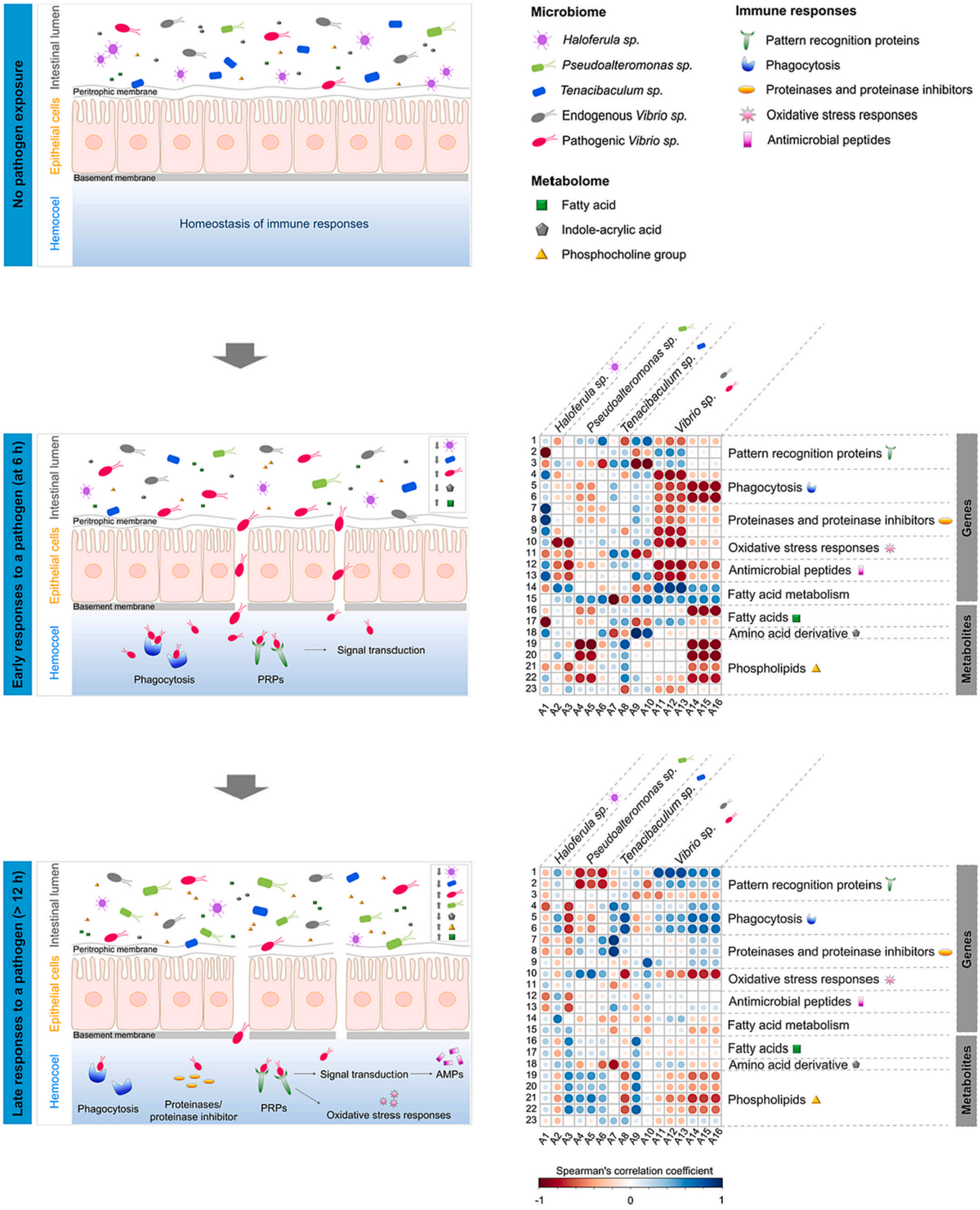

Fig. 7. Schematic model (left panel) and Spearman correlation analysis (right panel) of bacterial communities, host immune responses and metabolite profiles in *P. monodon* intestines upon the *V. harveyi* exposure. The correlation coefficient (|correlation coefficient| > 0.7) is represented by different colors (blue, positive correlation; red, negative correlation). The bacterial ASVs, DEGs, and metabolites ID are listed in Table S4. (For interpretation of the references to colour in this figure legend, the reader is referred to the web version of this article.)

findings are consistent with the previous studies in shrimp infected with white feces syndrome (WFS) (Huang et al., 2020) and acute hepatopancreatic necrosis disease (AHPND) (Hossain et al., 2021). The predominant phyla found in all shrimp intestines were Proteobacteria, Bacteroidetes, Planctomycetes and Verrucomicrobia, but their relative abundance at each time point after pathogen exposure was different. Among these phyla, Proteobacteria predominated in both unchallenged and challenged groups, consistent with the previous reports that Proteobacteria was the dominant phylum in the intestine of *P. monodon* and *L. vannamei* during *Vibrio* challenge (Rungrassamee et al., 2016; Zhang et al., 2021a). Proteobacteria are a commensal microflora and some members have been reported to be opportunistic pathogens in marine animals that can cause dysbiosis in intestinal microbiota (Holt et al., 2021). The relative abundance of genera *Haloferula* (phylum Verrucomicrobia) and *Tenacibaculum* (phylum Bacteroidetes) were significantly higher in the intestine of the unchallenged shrimp (0 h group), and these bacterial genera are commonly reported to be associated with healthy intestine of *P. monodon* (Chaiyapechara et al., 2022). The decrease in abundance of these bacteria after *V. harveyi* exposure could contribute to an imbalance in the gut microbiota, possibly due to the gut-derived infection. Moreover, several *Vibrio* ASVs associated with the shrimp intestine during pathogen exposure showed complex pattern, in which some *Vibrio* ASVs were found in significantly higher abundance in unexposed shrimp, while some *Vibrio* ASVs showed significantly higher abundance in the intestine at 6, 12 and 24 h after exposure to *V. harveyi*. To gain a better understanding of *Vibrio* dynamics during the pathogen exposure, we assigned these ASVs into *Vibrio* clades (Sawabe et al., 2013). The relative abundance of *Vibrio* ASVs related to Orientalis clade was high in the shrimp intestine at 0 h and decreased at the later time points after pathogen exposure. On the other hand, some *Vibrio* ASVs in the Harveyi and Vulnificus clades were found in higher abundance after bacterial exposure (6, 12 and 24 h). Most *Vibrio* species of the Orientalis clade have been reported as non-pathogenic bacteria for crustaceans, while members of the Harveyi clade and the Vulnificus clade were considered as important pathogenic bacteria such as *V. harveyi*, *V. parahaemolyticus,* and *V. vulnificus* (Restrepo et al., 2018). Hence, the higher abundance of *Vibrio* ASVs in the Harveyi and Vulnificus clades in response to the *V. harveyi* challenge could be viewed in as an indicator of an unhealthy state of the gut microbiota of shrimp. Interestingly, we found a shift in bacterial abundance toward *Pseudoalteromonas* in the intestines of the pathogen-exposed shrimp after 48 h. The involvement of *Pseudoalteromonas* needs further investigation to determine whether it is a transitional state to the recovery or to the secondary infection phase. Nevertheless, *Pseudoalteromonas* has been previously reported as a potential probiotic that produces antibacterial compounds to inhibit the growth of pathogens such as *V. parahaemolyticus* causing AHPND and *V. harveyi* (Radjasa et al., 2005; Wang et al., 2018). Therefore, higher abundance of this bacterial genus might help to maintain gut bacterial balance and improve immune system in shrimp. Despite its beneficial role, some strains of *Pseudoalteromonas* could also be opportunistic pathogens under stress condition (Ridgway et al., 2008; Tzuc et al., 2014). Interestingly, the observation of increasing abundance of *Pseudoalteromonas* is consistent with the previous report of gut bacterial communities in *L. vannamei* infected with WFS (Alfiansah et al., 2020). Therefore, an increase in *Pseudoalteromonas* species at 48 h after bacterial exposure could be indicative of secondary bacterial infection in shrimp.

As in other animals, the digestive organs of shrimp serve as an important entry point for pathogens that can lead to infection (Debnath et al., 2020; Soonthornchai et al., 2015), therefore, intestine of shrimp gut is the first line of defense against disease. Our study found that an exposure with *V. harveyi* modulated genes expression in the shrimp intestine, particularly the innate immune responses. The immune-related genes involved in phagocytosis, pattern recognition proteins (PRPs) and signal transduction were significantly up-regulated in response to early exposure (6 h group). In addition, genes associated with proteinases and proteinase inhibitors (PPIs), antimicrobial peptides (AMPs) and oxidative stress responses were differentially induced in the shrimp intestine. Phagocytosis is an important immune response for the clearance of pathogens in both vertebrates and invertebrates (Liu et al., 2020; Underhill and Ozinsky, 2002). Here, the transcripts of *low-density lipoprotein receptor-like*, *tubulin-specific chaperone cofactor E-like protein* and *peroxisomal sarcosine oxidase-like*, genes involved in the phagocytosis response (Liang et al., 2019; Rao et al., 2015; Wang et al., 2019a) were increased in the pathogen-exposed shrimp. Consistently, the expression of these genes has been reported to be increased during white spot syndrome virus (WSSV) infection in *L. vannamei* (Wang et al., 2019a). In crustaceans, pattern recognition proteins (PRPs) play an important role in the recognition of pathogen-associated molecular patterns (PAMPs) found on the surface of microorganisms and activate downstream immune responses such as AMPs, the prophenoloxidase (proPO) system, and melanization in response to pathogens (Jiravanichpaisal et al., 2006; Li and Xiang, 2013; Söderhäll and Cerenius, 1998). Our study also found that the members of PRP families such as *perlucin-like*, *ficolins,* and *c-type lectins* were significantly highly expressed in the intestine of shrimp in the early and late stages of the bacterial exposure. The transcription level of *perlucin-like protein* is inducible in *L. vannamei* after infection with *V. parahaemolyticus* and *V. anguillarum* (Bi et al., 2020). Moreover, c-type lectin-knockout of *P. monodon* showed higher shrimp mortality after *V. harveyi* challenge (Wongpanya et al., 2016), suggesting that immune-related genes involved in PRPs are important mediators of the initial induction of immune responses for host defense mechanisms against invading pathogens. In addition, genes involved in proteinases and proteinase inhibitors (PPIs) (e.g., *trypsin* and *trypsinogen*), signal transduction (*spätzle* and *ankyrin*), oxidative stress responses (*heat shock proteins*), AMPs (*lysozymes*) and other immune pathways (*astakines*) were stimulated at the later periods (12 to 48 h) of *V. harveyi* exposure. Ankyrins, along with the transcription factor Relish, play an important role in the immune deficiency (IMD) pathway, while Spätzles are key transcription factors in Toll pathway that recognize the specific pathogens (Tassanakajon et al., 2018). Activation of both pathways leads to the synthesis of AMPs in *Drosophila* (Kleino and Silverman, 2014; Valanne et al., 2011) and crustaceans including shrimp (Tassanakajon et al., 2018). Relish containing ankyrin repeat showed increased expression under *V. harveyi*, WSSV and yellow head virus (YHV) challenges in *P. monodon* (Tassanakajon et al., 2018; Visetnan et al., 2015). Similarly, the transcript level of *spätzle* was induced by *V. alginolyticus* and *Staphylococcus aureus*, which activate the production of AMPs in *L. vannamei* to eliminate bacteria (Yuan et al., 2017). AMPs are important for the innate immune system of shrimp and act as the first line of defense against invading pathogenic microbes (Tassanakajon et al., 2010). Here, the transcript levels of *lysozymes* belonging to the AMP families were increased at the later timepoint of *V. harveyi* exposure, and our observation was consistent with several previous studies in *P. monodon* (Somboonwiwat et al., 2006) and *L. stylirostris* (Destoumieux-Garzón et al., 2016). In addition, the transcript level of *astakine* increased in the intestine of pathogen-exposed shrimp. Astakine is an important cytokine involved in crustacean hematopoiesis. Astakines can stimulate new hemocytes, which play an important role in innate immune mechanisms to protect the host from invading microorganisms and in wound healing (Chang et al., 2013; Lin and Söderhäll, 2011). A previous study has reported increased protein expression of astakine in bacterial lipopolysaccharide (LPS)-injected *P. monodon* (Chang et al., 2013). Overall, our results suggest that up-regulation of immune-related genes associated with phagocytosis (e.g. *low-density lipoprotein receptor-like*, *tubulin-specific chaperone cofactor E-like protein* and *peroxisomal sarcosine oxidase-like*), PRPs (e.g. *perlucin-like*, *ficolins* and *c-type lectins*), PPIs (*trypsins* and *trypsinogens*), signal transduction (*spätzles* and *ankyrins*), oxidative stress responses (*heat shock proteins*), AMPs (*lysozymes*) were important for immune protection against pathogenic *V. harveyi* infection in shrimp.

In addition to immune responses, some energy- and metabolic-

related genes were also involved in *V. harveyi* exposed shrimp. Genes related to chitin metabolism were significantly up-regulated in the shrimp intestine at all time points of bacterial infection, such as *chitin binding domain*, *cuticle protein 2-like,* and *cuticle protein AM1159-like*. Chitin and cuticle protein are essential for the molting process, exoskeleton formation in crustaceans and part of peritrophic matrix (Nagasawa, 2012; Zhang et al., 2021b). Previous studies also show increased expression of genes encoding chitin and cuticle protein in *L. vannamei* infected with WSSV (Chen et al., 2021). These chitin and cuticle proteins can play a role in inhibiting the molting process, suggesting that the shrimp host are likely shifting much of its energetic balance toward immune defense mechanisms (Peruzza et al., 2020; Santos et al., 2020). Our result is consistent with this observation and corroborates the importance of chitin metabolism in maintaining homeostasis during pathogen exposure. Genes related to fatty acid metabolism such as *4-coumarate-CoA ligase 1*, *acetyl-CoA carboxy-like isoform X1,* and *fatty acid synthase-like* were up-regulated in the shrimp intestine after *V. harveyi* exposure. Among these, *fatty acid synthase-like* encoding an enzyme with a crucial role in lipid metabolism by regulating innate immune responses (Tzeng et al., 2019; Zuo et al., 2017) was significantly highly expressed at 24 and 48 h after the bacterial challenge. Consistently, the gene expression of fatty acid metabolism was reported to increase in *L. vannamei* after infection with *V. parahaemolyticus* (Zuo et al., 2017). Choline metabolism is a network of transporter systems and enzymes involved in choline-phospholipid metabolism and plays an essential role in the immune system (Snider et al., 2018). Here, several genes related to choline metabolism, such as *organic cation transporter proteins-like* and *solute carrier family 22 member 20-like*, were significantly expressed in the pathogen-exposed shrimp, suggesting that they were part of defense mechanisms against bacterial pathogen.

Interestingly, several significant patterns of metabolites were found in the shrimp intestine during the *V. harveyi* exposure. Based on an increased expression of the gene involved in choline metabolism after pathogenic bacteria challenge, this could lead to metabolite synthesis of phosphocholine groups (Inazu, 2019), which belong to phospholipid metabolites such as 1-(9Z-hexadecenoyl)-sn-glycero-3-phosphoethanolamine (LPE(16:1)), 1-[(9Z)-hexadecenoyl]-sn-glycero-3-phosphocholine (LPC(16:1/0:0)), L-α-lysophosphatidylcholine (L-α-LPC) and 2-oleoyl-sn-glycero-3-phosphocholine (LPC0:0/18:1) in shrimp at 24 and 48 h of the pathogen exposure. Previous studies have reported that LPC (16:1/0:0) and L-α-LPC can modulate antimicrobial activity against bacterial diseases (Aparna et al., 2012; Riessberger-Gallé et al., 2016). Phosphatidylcholine (PC) is not only an important component of the gastrointestinal tract (Ehehalt et al., 2010), but are also receiving increasing attention as protective agents in the gastrointestinal barrier, largely due to its roles in the formation of the hydrophobic surface of the colon (Korytowski et al., 2017). The accumulation of PC in the intestinal mucus layer plays a crucial role in protecting intestinal epithelia from the pathogenic bacterial invasion. Decreased phospholipids in colonic mucus have been associated with the development of ulcerative colitis, a chronic inflammatory bowel disease in human (Ehehalt et al., 2010; Korytowski et al., 2017). In addition, fatty acid metabolites can modulate immune responses by playing a role in anti-inflammation and reducing oxidative stress in human (Radzikowska et al., 2019) and aquatic animals (Natnan et al., 2021), playing a role in anti-inflammation and reducing oxidative stress. In addition to PC synthesized via choline metabolism, fatty acids can also produce PC through glycolysis pathway (Kwee and Lim, 2016). Moreover, some bacterial strains belonging to Proteobacteria can utilize fatty acid and phospholipid via the 3-oxoacyl-[acyl-carrier-protein] synthase 3 gene (*fab*H) (Hu and Cronan, 2020). Here, metabolites of α-linolenic acid, 13-hydroxy-9E,11E-octadecadienoic acid (13-HODE) and 8-hydroxyeicosapentaenoic acid (8-HEPE), members of the fatty acid metabolites were found in high concentration in the intestine of shrimp after bacterial exposure. On the other hand, we found that a group of metabolites related to amino acids and derivatives decreased after *V. harveyi* exposure including tryptophan and indole-3-acrylic acid. Indoles involve in regulating intestinal immune homeostasis during disease infection (Hendrikx and Schnabl, 2019). Previous reports have shown that some bacterial strains such as *Bacillus* sp., *Aeromonas* sp., *Fusobacterium* sp., *Shigella* sp. and *Vibrio* sp. can directly convert tryptophan to indole using the enzyme tryptophanase produced by bacteria (Agus et al., 2018; Lee and Lee, 2010). The low levels of tryptophan and indole-3-acrylic acid might be due to dysbiosis of the gut microbiota by bacterial pathogen possibly leading to a reduction in some *Vibrio* species associated with clades Orientalis, Harveyi and Vulnificus that can produce metabolites of indole group (Lee and Lee, 2010). In addition, we also found a group of metabolites involved in purines/pyrimidines and derivatives decreased after the *V. harveyi* exposure. Purines and pyrimidines play important roles in cell cycle, cell proliferation, and immune response in human (Quéméneur et al., 2003; Yin et al., 2018). Our observation might due to the decreased expression of the genes involved in purine/pyrimidine synthesis, such as *xanthine dehydrogenase/oxidase-like* (Tani et al., 2019), leading to a decrease in metabolite levels.

The pathogenic *V. harveyi* affected the microbiota, host gene expressions and metabolite patterns in the intestine of *P. monodon*. The schematic model derived from our multi-omics analysis (Fig. 7 and Table S4) shows the state of homeostasis under non-pathogenic exposure, where shrimp could maintain normal healthy ranges for factors such as energy intake, growth, and innate immune system. Under normal circumstances, the intestinal microbiota was formed and established their niches in the shrimp intestine. However, an exposure to a pathogenic *V. harveyi* could lead to alteration of intestinal microbial communities. Here, *Vibrio* ASVs increased with *V. harveyi* exposure, while abundance of bacterial groups such as *Haloferula* sp. and *Tenacibaculum* sp. became decreased. Immune responses such as phagocytosis, PRPs, and signal transduction were stimulated in the shrimp intestine at the beginning of the exposure (6 h). In addition, metabolite levels showed an increase in phospholipids and fatty acids in the intestine of shrimp after pathogen exposure. The presence of pathogenic *V. harveyi* correlated negatively with the expression of immune-related genes and the levels of host metabolites to cope with pathogen invasion. However, stimulation of immune responses could affect the relative abundance of other bacterial genera such as *Haloferula* and *Tenacibaculum*, which was consistent with our bacterial co-occurrence analysis showing a shift in bacterial network at 6 h of the pathogen exposure (Fig. 4C). In the later phase of bacterial exposure (12 to 48 h), several gene-related immune pathways were induced, including phagocytosis, PPIs, PRPs, signal transduction, AMPs and oxidative stress responses after pathogen challenge. The negative correlation between *Vibrio* and metabolites, including fatty acids and phospholipids was observed in late responses to exposure to the pathogenic *V. harveyi*, whereas *Pseudoalteromonas* showed the opposite pattern of this metabolite correlation, suggesting that fatty acid and phospholipid metabolites might not affect abundance of *Pseudoalteromonas*. This result may explain the increasing negative correlations between *Vibrio* ASVs and *Pseudoalteromonas* ASVs at 24 h observed in our co-occurrence network analysis (Fig. 4E) and resulted in a significant increase in *Pseudoalteromonas* at 48 h after pathogen challenge. Our observations suggest that the exposure of *V. harveyi* resulted in changes in bacterial communities, molecular mechanisms, especially innate immune responses, and metabolite compounds in the shrimp intestine as a consequence of the presence of a pathogen and activated host responses to such a pathogen. As a matter of fact, the host organism and its microbiota actually have a two-way relationship, in which changes in the host gene expression profile influence the microbial composition and vice versa (Nichols and Davenport, 2021). Moreover, it is still difficult to determine whether the metabolites identified in our study were entirely derived from the pathogen and the gut microbiota or from other sources such as diet or the host shrimp itself. To unravel this complex relationship, it may be useful in the future to perform a metagenomic analysis along with a metabolomic study to identify metabolites that may be potentially derived from the shrimp gut

microbiome. Furthermore, an in vivo system such as a germ-free model will provide greater insight into shrimp-gut microbial interactions. However, compared to model organisms such as the mouse, zebrafish, and fruit fly, the black tiger shrimp, which is a non-model organism, has limited tools to study host-microbial interactions (Zhang et al., 2020a). To gain further insight into the interactions between shrimp and microbiota, the development of a germ-free system for black tiger shrimp will be an indispensable tool to understand the direction of causality between host factors and environmental conditions on microbial composition.

5. Conclusion

As an aquatic organism, shrimp are susceptible to ingestion of opportunistic bacterial pathogens from their environment such as rearing water, feed, and pond sediment. Integrative analysis of gut microbiota, host responses, and metabolite profiles can help to understand comprehensive changes in host's physiological state in the presence of a pathogen. The shift in bacterial communities was observed in our study, suggesting that *V. harveyi* perturbed the composition of the intestinal microbiota. Gene expression in the shrimp intestine including those involved in the immune system and energy metabolism showed differential expression during *V. harveyi* challenge. Several immune responses such as phagocytosis, PRPs, PPIs, signal transduction and AMPs against invading pathogen were stimulated. In addition, higher concentration of phospholipid groups and fatty acids in the later phase of an exposure could contribute to maintaining the intestinal homeostasis of shrimp. The integrative study of intestinal microbiota, metabolites and host gene expression shed light on host-gut microbial interactions in shrimp upon a presence of a bacterial pathogen. Further studies on how metabolites mediate the interaction between gut bacteria and host shrimp will be essential to understand host's physiological condition under the interference.

Supplementary data to this article can be found online at https://doi.org/10.1016/j.aquaculture.2023.739252.

Author contributions

The authors confirm contribution to the paper as follows: study conception and design: WR, SC, NK; animal trial: MP, SC, WR, PA, SA; data collection: PA, UU, WR; data analysis: TU, UU, WR, JK, PS, VS; interpretation of results: WR, PA, TU; draft manuscript preparation: PA, WR. All authors read and approved the submitted version of the manuscript.

Funding

This project was supported by National Center for Genetic Engineering and Biotechnology (BIOTEC Grant No. P1652214) and the European Union's Horizon 2020 Research and Innovation Program under the Marie Skłodowska-Curie grant agreement No 734486 (SAFE-Aqua).

Declaration of Competing Interest

The authors declare that they have no known competing financial interests or personal relationships that could have appeared to influence the work reported in this paper.

Data availability

Microbiome and RNA-seq data generated in this study are available under NCBI BioProject number PRJNA689097. Metabolite data can be found in supplementary Table S5.

Acknowledgments

We thank Dr. Anavaj Sakuntabhai from Pasteur Institute (France) for his advice and suggestion on transcriptomic data analysis. We are truly grateful to Prof. Morakot Tanticharoen (NSTDA, Thailand), Dr. Kanyawim Kirtikara (BIOTEC, Thailand), and Dr. Wonnop Visessanguan (BIOTEC, Thailand) for their mentorship and guidance on the shrimp research program.

References

Agus, A., Planchais, J., Sokol, H., 2018. Gut microbiota regulation of tryptophan metabolism in health and disease. Cell Host Microbe 23 (6), 716–724. https://doi.org/10.1016/j.chom.2018.05.003.

Alfiansah, Y.R., Peters, S., Harder, J., Hassenrück, C., Gärdes, A., 2020. Structure and co-occurrence patterns of bacterial communities associated with white faeces disease outbreaks in Pacific white-leg shrimp *Penaeus vannamei* aquaculture. Sci. Rep. 10 (1), 11980. https://doi.org/10.1038/s41598-020-68891-6.

Angthong, P., Roytrakul, S., Jarayabhand, P., Jiravanichpaisal, P., 2017. Characterization and function of a tachylectin 5-like immune molecule in *Penaeus monodon*. Dev. Comp. Immunol. 76 https://doi.org/10.1016/j.dci.2017.05.023.

Angthong, P., Uengwetwanit, T., Arayamethakorn, S., Chaitongsakul, P., Karoonuthaisiri, N., Rungrassamee, W., 2020. Bacterial analysis in the early developmental stages of the black tiger shrimp (*Penaeus monodon*). Sci. Rep. 10 (1), 4896. https://doi.org/10.1038/s41598-020-61559-1.

Aparna, V., Dileep, K.V., Mandal, P.K., Karthe, P., Sadasivan, C., Haridas, M., 2012. Anti-inflammatory property of n-hexadecanoic acid: structural evidence and kinetic assessment. Chem. Biol. Drug Des. 80 (3), 434–439. https://doi.org/10.1111/j.1747-0285.2012.01418.x.

Bai, S., Yao, Z., Raza, M.F., Cai, Z., Zhang, H., 2021. Regulatory mechanisms of microbial homeostasis in insect gut. Insect Sci. 28 (2), 286–301. https://doi.org/10.1111/1744-7917.12868.

Bi, J., Ning, M., Xie, X., Fan, W., Huang, Y., Gu, W., Wang, W., Wang, L., Meng, Q., 2020. A typical C-type lectin, perlucin-like protein, is involved in the innate immune defense of whiteleg shrimp *Litopenaeus vannamei*. Fish. Shellfish. Immunol. 103, 293–301. https://doi.org/10.1016/j.fsi.2020.05.046.

Bolyen, E., Rideout, J.R., Dillon, M.R., Bokulich, N.A., Abnet, C.C., Al-Ghalith, G.A., Alexander, H., Alm, E.J., Arumugam, M., Asnicar, F., Bai, Y., Bisanz, J.E., Bittinger, K., Brejnrod, A., Brislawn, C.J., Brown, C.T., Callahan, B.J., Caraballo-Rodríguez, A.M., Chase, J., Cope, E.K., Da Silva, R., Diener, C., Dorrestein, P.C., Douglas, G.M., Durall, D.M., Duvallet, C., Edwardson, C.F., Ernst, M., Estaki, M., Fouquier, J., Gauglitz, J.M., Gibbons, S.M., Gibson, D.L., Gonzalez, A., Gorlick, K., Guo, J., Hillmann, B., Holmes, S., Holste, H., Huttenhower, C., Huttley, G.A., Janssen, S., Jarmusch, A.K., Jiang, L., Kaehler, B.D., Kang, K.B., Keefe, C.R., Keim, P., Kelley, S.T., Knights, D., Koester, I., Kosciolek, T., Kreps, J., Langille, M.G.I., Lee, J., Ley, R., Liu, Y.-X., Loftfield, E., Lozupone, C., Maher, M., Marotz, C., Martin, B.D., McDonald, D., McIver, L.J., Melnik, A.V., Metcalf, J.L., Morgan, S.C., Morton, J.T., Naimey, A.T., Navas-Molina, J.A., Nothias, L.F., Orchanian, S.B., Pearson, T., Peoples, S.L., Petras, D., Preuss, M.L., Pruesse, E., Rasmussen, L.B., Rivers, A., Robeson, M.S., Rosenthal, P., Segata, N., Shaffer, M., Shiffer, A., Sinha, R., Song, S.J., Spear, J.R., Swafford, A.D., Thompson, L.R., Torres, P.J., Trinh, P., Tripathi, A., Turnbaugh, P.J., Ul-Hasan, S., van der Hooft, J.J.J., Vargas, F., Vázquez-Baeza, Y., Vogtmann, E., von Hippel, M., Walters, W., Wan, Y., Wang, M., Warren, J., Weber, K.C., Williamson, C.H.D., Willis, A.D., Xu, Z.Z., Zaneveld, J.R., Zhang, Y., Zhu, Q., Knight, R., Caporaso, J.G., 2019. Reproducible, interactive, scalable and extensible microbiome data science using QIIME 2. Nat. Biotechnol. 37 (8), 852–857. https://doi.org/10.1038/s41587-019-0209-9.

Callahan, B.J., McMurdie, P.J., Rosen, M.J., Han, A.W., Johnson, A.J.A., Holmes, S.P., 2016. DADA2: high-resolution sample inference from Illumina amplicon data. Nat. Methods 13 (7), 581–583. https://doi.org/10.1038/nmeth.3869.

Camacho, C., Coulouris, G., Avagyan, V., Ma, N., Papadopoulos, J., Bealer, K., Madden, T.L., 2009. BLAST+: architecture and applications. BMC Bioinform. 10 (1), 421. https://doi.org/10.1186/1471-2105-10-421.

Chaiyapechara, S., Uengwetwanit, T., Arayamethakorn, S., Bunphimpapha, P., Phromson, M., Jangsutthivorawat, W., Tala, S., Karoonuthaisiri, N., Rungrassamee, W., 2022. Understanding the host-microbe-environment interactions: intestinal microbiota and transcriptomes of black tiger shrimp *Penaeus monodon* at different salinity levels. Aquaculture 546, 737371. https://doi.org/10.1016/j.aquaculture.2021.737371.

Chang, Y.T., Lin, C.Y., Tsai, C.Y., Siva, V.S., Chu, C.Y., Tsai, H.J., Song, Y.L., 2013. The new face of the old molecules: crustin Pm4 and transglutaminase type I serving as rnps down-regulate astakine-mediated hematopoiesis. PLoS One 8 (8), e72793. https://doi.org/10.1371/journal.pone.0072793.

Chen, Y.L., Kumar, R., Liu, C.H., Wang, H.C., 2021. In *Litopenaeus vannamei*, the cuticular chitin-binding proteins LvDD9A and LvDD9B retard AHPND pathogenesis but facilitate WSSV infection. Dev. Comp. Immunol. 120, 103999 https://doi.org/10.1016/j.dci.2021.103999.

Davoodi, S., Foley, E., 2020. Host-microbe-pathogen interactions: a review of *Vibrio cholerae* pathogenesis in *Drosophila*. Front. Immunol. 10 (3128) https://doi.org/10.3389/fimmu.2019.03128.

de Souza Valente, C., Wan, A.H.L., 2021. Vibrio and major commercially important vibriosis diseases in decapod crustaceans. J. Invertebr. Pathol. 181, 107527 https://doi.org/10.1016/j.jip.2020.107527.

Debnath, A., Mizuno, T., Miyoshi, S.-I., 2020. Regulation of chitin-dependent growth and natural competence in *Vibrio parahaemolyticus*. Microorganisms 8 (9), 1303. https://doi.org/10.3390/microorganisms8091303.

Destoumieux-Garzón, D., Rosa, R.D., Schmitt, P., Barreto, C., Vidal-Dupiol, J., Mitta, G., Gueguen, Y., Bachère, E., 2016. Antimicrobial peptides in marine invertebrate health and disease. Philos. Trans. R. Soc. Lond. Ser. B Biol. Sci. 371 (1695), 20150300. https://doi.org/10.1098/rstb.2015.0300.

Dobin, A., Davis, C.A., Schlesinger, F., Drenkow, J., Zaleski, C., Jha, S., Batut, P., Chaisson, M., Gingeras, T.R., 2012. STAR: ultrafast universal RNA-seq aligner. Bioinformatics 29 (1), 15–21. https://doi.org/10.1093/bioinformatics/bts635.

Duan, Y., Wang, Y., Dong, H., Ding, X., Liu, Q., Li, H., Zhang, J., Xiong, D., 2018. Changes in the intestine microbial, digestive, and immune-related genes of *Litopenaeus vannamei* in response to dietary probiotic *clostridium butyricum* supplementation. Front. Microbiol. 9, 2191. https://doi.org/10.3389/fmicb.2018.02191.

Duan, Y., Xiong, D., Wang, Y., Li, H., Dong, H., Zhang, J., 2021. Toxic effects of ammonia and thermal stress on the intestinal microbiota and transcriptomic and metabolomic responses of *Litopenaeus vannamei*. Sci. Total Environ. 754, 141867 https://doi.org/10.1016/j.scitotenv.2020.141867.

Ehehalt, R., Braun, A., Karner, M., Füllekrug, J., Stremmel, W., 2010. Phosphatidylcholine as a constituent in the colonic mucosal barrier–physiological and clinical relevance. Biochim. Biophys. Acta 1801 (9), 983–993. https://doi.org/10.1016/j.bbalip.2010.05.014.

Fabregat, A., Sidiropoulos, K., Garapati, P., Gillespie, M., Hausmann, K., Haw, R., Jassal, B., Jupe, S., Korninger, F., McKay, S., Matthews, L., May, B., Milacic, M., Rothfels, K., Shamovsky, V., Webber, M., Weiser, J., Williams, M., Wu, G., Stein, L., Hermjakob, H., D'Eustachio, P., 2016. The reactome pathway knowledgebase. Nucleic Acids Res. 44 (D1), D481–D487. https://doi.org/10.1093/nar/gkv1351.

FAO, 2016. Food and Agriculture Organization of the United Nations Statistics. Fisheries and Aquaculture Software. FishStat Plus - Universal Software for Fishery Statistical Time Series. Fisheries and Aquaculture Department, Rome.

Faust, K., Raes, J., 2012. Microbial interactions: from networks to models. Nat. Rev. Microbiol. 10 (8), 538–550. https://doi.org/10.1038/nrmicro2832.

Faust, K., Raes, J., 2016. CoNet app: inference of biological association networks using Cytoscape. F1000Research 5, 1519. https://doi.org/10.12688/f1000research.9050.2.

Flegel, T., 2019. A future vision for disease control in shrimp aquaculture. J. World Aquacult. Soc. 50 https://doi.org/10.1111/jwas.12589.

Götz, S., García-Gómez, J.M., Terol, J., Williams, T.D., Nagaraj, S.H., Nueda, M.J., Robles, M., Talón, M., Dopazo, J., Conesa, A., 2008. High-throughput functional annotation and data mining with the Blast2GO suite. Nucleic Acids Res. 36 (10), 3420–3435. https://doi.org/10.1093/nar/gkn176.

Hanning, I., Diaz-Sanchez, S., 2015. The functionality of the gastrointestinal microbiome in non-human animals. Microbiome 3, 51. https://doi.org/10.1186/s40168-015-0113-6.

Harrell, J.F., Dupont, C., 2019. Hmisc: Harrell Miscellaneous. R Package Version 4.2-0. CRAN.R-project.org/package=Hmisc.

Hegedus, D., Erlandson, M., Gillott, C., Toprak, U., 2009. New insights into peritrophic matrix synthesis, architecture, and function. Annu. Rev. Entomol. 54, 285–302. https://doi.org/10.1146/annurev.ento.54.110807.090559.

Hendrikx, T., Schnabl, B., 2019. Indoles: metabolites produced by intestinal bacteria capable of controlling liver disease manifestation. J. Intern. Med. 286 https://doi.org/10.1111/joim.12892.

Holt, C.C., Bass, D., Stentiford, G.D., van der Giezen, M., 2021. Understanding the role of the shrimp gut microbiome in health and disease. J. Invertebr. Pathol. 186, 107387 https://doi.org/10.1016/j.jip.2020.107387.

Hoseinifar, S.H., Eshaghzadeh, H., Vahabzadeh Roodsari, H., Peykaran, N., 2015. Modulation of growth performances, survival, digestive enzyme activities and intestinal microbiota in common carp (*Cyprinus carpio*) larvae using short chain fructooligosaccharide. Aquac. Res. 47 https://doi.org/10.1111/are.12777.

Hossain, M.S., Dai, J., Qiu, D., 2021. Dysbiosis of the shrimp (*Penaeus monodon*) gut microbiome with AHPND outbreaks revealed by 16S rRNA metagenomics analysis. Aquac. Res. 52 https://doi.org/10.1111/are.15178.

Hu, Y., Cronan, J.E., 2020. α-proteobacteria synthesize biotin precursor pimeloyl-ACP using BioZ 3-ketoacyl-ACP synthase and lysine catabolism. Nat. Commun. 11 (1), 5598. https://doi.org/10.1038/s41467-020-19251-5.

Huang, Z., Zeng, S., Hou, D., Zhou, R., Xing, C., Wei, D., Deng, X., Yu, L., Wang, H., Deng, Z., Weng, S., Sataporncanit, K., Ning, D., Zhou, J., He, J., 2020. Microecological Koch's postulates reveal that intestinal microbiota dysbiosis contributes to shrimp white feces syndrome. Microbiome 8. https://doi.org/10.1186/s40168-020-00802-3.

Huerta-Cepas, J., Szklarczyk, D., Heller, D., Hernández-Plaza, A., Forslund, S.K., Cook, H., Mende, D.R., Letunic, I., Rattei, T., Jensen, L.J., von Mering, C., Bork, P., 2019. eggNOG 5.0: a hierarchical, functionally and phylogenetically annotated orthology resource based on 5090 organisms and 2502 viruses. Nucleic Acids Res. 47 (D1), D309–d314. https://doi.org/10.1093/nar/gky1085.

Inazu, M., 2019. Functional expression of choline transporters in the blood–brain barrier. Nutrients 11, 2265. https://doi.org/10.3390/nu11102265.

Jiravanichpaisal, P., Lee, B.L., Söderhäll, K., 2006. Cell-mediated immunity in arthropods: hematopoiesis, coagulation, melanization and opsonization. Immunobiology 211 (4), 213–236. https://doi.org/10.1016/j.imbio.2005.10.015.

Jukes, T.H., Cantor, C.R., 1969. Chapter 24-Evolution of protein molecules. In: Munro, H. N. (Ed.), Mammalian protein metabolism. Academic Press, New York.

Kalaimani, N., Thiagarajan, R., Chakravarthy, N., Raja, S., Ponniah, A.G., 2013. Economic losses due to disease incidences in shrimp farms of India. Fish. Technol. 50, 80–86.

Kewcharoen, W., Srisapoome, P., 2019. Probiotic effects of *Bacillus spp.* from Pacific white shrimp (*Litopenaeus vannamei*) on water quality and shrimp growth, immune responses, and resistance to *Vibrio parahaemolyticus* (AHPND strains). Fish. Shellfish. Immunol. 94, 175–189. https://doi.org/10.1016/j.fsi.2019.09.013.

Kleino, A., Silverman, N., 2014. The *Drosophila* IMD pathway in the activation of the humoral immune response. Dev. Comp. Immunol. 42 (1), 25–35. https://doi.org/10.1016/j.dci.2013.05.014.

Kongnum, K., Hongpattarakere, T., 2012. Effect of *Lactobacillus plantarum* isolated from digestive tract of wild shrimp on growth and survival of white shrimp (*Litopenaeus vannamei*) challenged with *Vibrio harveyi*. Fish. Shellfish. Immunol. 32 (1), 170–177. https://doi.org/10.1016/j.fsi.2011.11.008.

Korytowski, A., Abuillan, W., Amadei, F., Makky, A., Gumiero, A., Sinning, I., Gauss, A., Stremmel, W., Tanaka, M., 2017. Accumulation of phosphatidylcholine on gut mucosal surface is not dominated by electrostatic interactions. Biochim. Biophys. Acta 1859 (5), 959–965. https://doi.org/10.1016/j.bbamem.2017.02.008.

Kounatidis, I., Ligoxygakis, P., 2012. *Drosophila* as a model system to unravel the layers of innate immunity to infection. Open Biol. 2 (5), 120075 https://doi.org/10.1098/rsob.120075.

Krueger, F., Frankie James, F., Ewels, P., Afyounian, E., Schuster-Boeckler, B., 2021. FelixKrueger/TrimGalore: v0.6.7. Zenodo. https://doi.org/10.5281/zenodo.5127899.

Kumar, S., Stecher, G., Li, M., Knyaz, C., Tamura, K., 2018. MEGA X: molecular evolutionary genetics analysis across computing platforms. Mol. Biol. Evol. 35 (6), 1547–1549. https://doi.org/10.1093/molbev/msy096.

Kuraishi, T., Hori, A., Kurata, S., 2013. Host-microbe interactions in the gut of *Drosophila melanogaster*. Front. Physiol. 4, 375. https://doi.org/10.3389/fphys.2013.00375.

Kwee, S.A., Lim, J., 2016. Metabolic positron emission tomography imaging of cancer: pairing lipid metabolism with glycolysis. World J. Radiol. 8 (11), 851–856. https://doi.org/10.4329/wjr.v8.i11.851.

Lee, J.H., Lee, J., 2010. Indole as an intercellular signal in microbial communities. FEMS Microbiol. Rev. 34 (4), 426–444. https://doi.org/10.1111/j.1574-6976.2009.00204.x.

Li, F., Xiang, J., 2013. Recent advances in researches on the innate immunity of shrimp in China. Dev. Comp. Immunol. 39 (1–2), 11–26. https://doi.org/10.1016/j.dci.2012.03.016.

Liang, Z., Yang, L., Zheng, J., Zuo, H., Weng, S., He, J., Xu, X., 2019. A low-density lipoprotein receptor (LDLR) class A domain-containing C-type lectin from *Litopenaeus vannamei* plays opposite roles in antibacterial and antiviral responses. Dev. Comp. Immunol. 92, 29–34. https://doi.org/10.1016/j.dci.2018.11.002.

Liao, Y., Smyth, G.K., Shi, W., 2014. featureCounts: an efficient general purpose program for assigning sequence reads to genomic features. Bioinformatics 30 (7), 923–930. https://doi.org/10.1093/bioinformatics/btt656.

Lin, X., Söderhäll, I., 2011. Crustacean hematopoiesis and the astakine cytokines. Blood 117, 6417–6424. https://doi.org/10.1182/blood-2010-11-320614.

Liu, S., Zheng, S.-C., Li, Y.-L., Li, J., Liu, H.-P., 2020. Hemocyte-mediated phagocytosis in crustaceans. Front. Immunol. 11, 268. https://doi.org/10.3389/fimmu.2020.00268.

Livak, K.J., Schmittgen, T.D., 2001. Method analysis of relative gene expression data using real-time quantitative PCR and the $2^{-\Delta\Delta CT}$ method. Methods 25 (4), 402–408. https://doi.org/10.1006/meth.2001.1262.

Love, M.I., Huber, W., Anders, S., 2014. Moderated estimation of fold change and dispersion for RNA-seq data with DESeq2. Genome Biol. 15 (12), 550. https://doi.org/10.1186/s13059-014-0550-8.

McMurdie, P.J., Holmes, S., 2013. phyloseq: an R package for reproducible interactive analysis and graphics of microbiome census data. PLoS One 8 (4), e61217. https://doi.org/10.1371/journal.pone.0061217.

Montgomery, M.T., Kirchman, D.L., 1993. Role of chitin-binding proteins in the specific attachment of the marine bacterium *Vibrio harveyi* to chitin. Appl. Environ. Microbiol. 59 (2), 373–379. https://doi.org/10.1128/aem.59.2.373-379.1993.

Muthukrishnan, S., Defoirdt, T., Ina-Salwany, M.Y., Yusoff, F.M., Shariff, M., Ismail, S.I., Natrah, I., 2019. *Vibrio parahaemolyticus* and *Vibrio harveyi* causing Acute Hepatopancreatic Necrosis Disease (AHPND) in *Penaeus vannamei* (Boone, 1931) isolated from Malaysian shrimp ponds. Aquaculture 511, 734227. https://doi.org/10.1016/j.aquaculture.2019.734227.

Nagasawa, H., 2012. The crustacean cuticle: structure, composition and mineralization. Front. Biosci. (Elite Ed) 4, 711–720. https://doi.org/10.2741/E412.

Natnan, M.E., Mayalvanan, Y., Jazamuddin, F.M., Aizat, W.M., Low, C.-F., Goh, H.-H., Azizan, K.A., Bunawan, H., Baharum, S.N., 2021. Omics strategies in current advancements of infectious fish disease management. Biology 10 (11), 1086.

Nichols, R.G., Davenport, E.R., 2021. The relationship between the gut microbiome and host gene expression: a review. Hum. Genet. 140 (5), 747–760. https://doi.org/10.1007/s00439-020-02237-0.

Pérez, T., Balcázar, J.L., Ruiz-Zarzuela, I., Halaihel, N., Vendrell, D., de Blas, I., Múzquiz, J.L., 2010. Host–microbiota interactions within the fish intestinal ecosystem. Mucosal Immunol. 3 (4), 355–360. https://doi.org/10.1038/mi.2010.12.

Peruzza, L., Thamizhvanan, S., Vimal, S., Vinaya Kumar, K., Shekhar, M.S., Smith, V.J., Hauton, C., Vijayan, K.K., Sahul Hameed, A.S., 2020. A comparative synthesis of transcriptomic analyses reveals major differences between WSSV-susceptible *Litopenaeus vannamei* and WSSV-refractory *Macrobrachium rosenbergii*. Dev. Comp. Immunol. 104, 103564 https://doi.org/10.1016/j.dci.2019.103564.

Quast, C., Pruesse, E., Yilmaz, P., Gerken, J., Schweer, T., Yarza, P., Peplies, J., Glöckner, F.O., 2013. The SILVA ribosomal RNA gene database project: improved data processing and web-based tools. Nucleic Acids Res. 41 (Database issue), D590–D596. https://doi.org/10.1093/nar/gks1219.

Quéméneur, L., Gerland, L.-M., Flacher, M., Ffrench, M., Revillard, J.-P., Genestier, L., 2003. Differential control of cell cycle, proliferation, and survival of primary T

lymphocytes by purine and pyrimidine nucleotides. J. Immunol. 170 (10), 4986–4995. https://doi.org/10.4049/jimmunol.170.10.4986.
R Core Team, 2020. R: A Language and Environment for Statistical Computing. R Foundation for Statistical Computing, Vienna, Austria.
Radjasa, O.K., Martens, T., Grossart, H.-P., Sabdono, A., Simon, M., Bachtiar, T., 2005. Antibacterial property of a aoral-associated bacterium *Pseudoalteromonas luteoviolacea* against shrimp pathogenic *Vibrio harveyi* (*in vitro* study). HAYATI J. Biosci. 12 (2), 77–81. https://doi.org/10.1016/S1978-3019(16)30329-1.
Radzikowska, U., Rinaldi, A.O., Çelebi Sözener, Z., Karaguzel, D., Wojcik, M., Cypryk, K., Akdis, M., Akdis, C.A., Sokolowska, M., 2019. The influence of dietary fatty acids on immune responses. Nutrients 11 (12), 2990. https://doi.org/10.3390/nu11122990.
Rajeev, R., Adithya, K.K., Kiran, S., Selvin, J., 2020. Healthy microbiome: a key to successful and sustainable shrimp aquaculture. Rev. Aquac. 13 https://doi.org/10.1111/raq.12471.
Rao, R., Bing Zhu, Y., Alinejad, T., Tiruvayipati, S., Lin Thong, K., Wang, J., Bhassu, S., 2015. RNA-seq analysis of *Macrobrachium rosenbergii* hepatopancreas in response to *Vibrio parahaemolyticus* infection. Gut Pathog. 7 (1), 6. https://doi.org/10.1186/s13099-015-0052-6.
Restrepo, L., Bayot, B., Arciniegas, S., Bajaña, L., Betancourt, I., Panchana, F., Reyes Muñoz, A., 2018. PirVP genes causing AHPND identified in a new *Vibrio* species (*Vibrio punensis*) within the commensal *Orientalis* clade. Sci. Rep. 8 (1), 13080. https://doi.org/10.1038/s41598-018-30903-x.
Reveco, F.E., Øverland, M., Romarheim, O.H., Mydland, L.T., 2014. Intestinal bacterial community structure differs between healthy and inflamed intestines in Atlantic salmon (*Salmo salar* L.). Aquaculture 420-421, 262–269. https://doi.org/10.1016/j.aquaculture.2013.11.007.
Ridgway, I.D., Small, H.J., Atkinson, R.J.A., Birkbeck, H.T., Taylor, A.C., Neil, D.M., 2008. Extracellular proteases and possible disease related virulence mechanisms of two marine bacteria implicated in an opportunistic bacterial infection of *Nephrops norvegicus*. J. Invertebr. Pathol. 99 (1), 14–19. https://doi.org/10.1016/j.jip.2008.05.007.
Riessberger-Gallé, U., Hernández-López, J., Rechberger, G., Crailsheim, K., Schuehly, W., 2016. Lysophosphatidylcholine acts in the constitutive immune defence against American foulbrood in adult honeybees. Sci. Rep. 6, 30699. https://doi.org/10.1038/srep30699.
RStudio Team, 2020. RStudio: Integrated Development for R. RStudio, PBC, Boston, MA.
Rungrassamee, W., Klanchui, A., Maibunkaew, S., Chaiyapechara, S., Jiravanichpaisal, P., Karoonuthaisiri, N., 2014. Characterization of intestinal bacteria in wild and domesticated adult black tiger shrimp (*Penaeus monodon*). PLoS One 9 (3), e91853. https://doi.org/10.1371/journal.pone.0091853.
Rungrassamee, W., Klanchui, A., Maibunkaew, S., Karoonuthaisiri, N., 2016. Bacterial dynamics in intestines of the black tiger shrimp and the Pacific white shrimp during *Vibrio harveyi* exposure. J. Invertebr. Pathol. 133, 12–19. https://doi.org/10.1016/j.jip.2015.11.004.
Santos, C.A., Andrade, S.C.S., Fernandes, J.M.O., Freitas, P.D., 2020. Shedding the light on *Litopenaeus vannamei* differential muscle and hepatopancreas immune responses in white spot syndrome virus (WSSV) exposure. Genes (Basel) 11 (7), 805. https://doi.org/10.3390/genes11070805.
Sawabe, T., Ogura, Y., Matsumura, Y., Feng, G., Amin, A.R., Mino, S., Nakagawa, S., Sawabe, T., Kumar, R., Fukui, Y., Satomi, M., Matsushima, R., Thompson, F.L., Gomez-Gil, B., Christen, R., Maruyama, F., Kurokawa, K., Hayashi, T., 2013. Updating the *Vibrio* clades defined by multilocus sequence phylogeny: proposal of eight new clades, and the description of *Vibrio tritonius sp*. nov. Front. Microbiol. 4, 414. https://doi.org/10.3389/fmicb.2013.00414.
Segata, N., Izard, J., Waldron, L., Gevers, D., Miropolsky, L., Garrett, W.S., Huttenhower, C., 2011. Metagenomic biomarker discovery and explanation. Genome Biol. 12 (6), R60. https://doi.org/10.1186/gb-2011-12-6-r60.
Sehnal, L., Brammer-Robbins, E., Wormington, A.M., Blaha, L., Bisesi, J., Larkin, I., Martyniuk, C.J., Simonin, M., Adamovsky, O., 2021. Microbiome composition and function in aquatic vertebrates: small organisms making big impacts on aquatic animal health. Front. Microbiol. 12 (358) https://doi.org/10.3389/fmicb.2021.567408.
Shannon, P., Markiel, A., Ozier, O., Baliga, N.S., Wang, J.T., Ramage, D., Amin, N., Schwikowski, B., Ideker, T., 2003. Cytoscape: a software environment for integrated models of biomolecular interaction networks. Genome Res. 13 (11), 2498–2504. https://doi.org/10.1101/gr.1239303.
Silveira, A.S., Matos, G.M., Falchetti, M., Ribeiro, F.S., Bressan, A., Bachère, E., Perazzolo, L.M., Rosa, R.D., 2018. An immune-related gene expression atlas of the shrimp digestive system in response to two major pathogens brings insights into the involvement of hemocytes in gut immunity. Dev. Comp. Immunol. 79, 44–50. https://doi.org/10.1016/j.dci.2017.10.005.
Snider, S., Margison, K., Ghorbani, P., Leblond, N., O'Dwyer, C., Nunes, J., Nguyen, T., Xu, H., Bennett, S., Fullerton, M., 2018. Choline transport links macrophage phospholipid metabolism and inflammation. J. Biol. Chem. 293 https://doi.org/10.1074/jbc.RA118.003180 jbc.RA118.003180.
Söderhäll, K., Cerenius, L., 1998. Role of the prophenoloxidase-activating system in invertebrate immunity. Curr. Opin. Dent. 10 (1), 23–28. https://doi.org/10.1016/S0952-7915(98)80026-5.
Somboonwiwat, K., Supungul, P., Rimphanitchayakit, V., Aoki, T., Hirono, I., Tassanakajon, A., 2006. Differentially expressed genes in hemocytes of *Vibrio harveyi*-challenged shrimp *Penaeus monodon*. J. Biochem. Mol. Biol. 39 (1), 26–36. https://doi.org/10.5483/bmbrep.2006.39.1.026.
Soonthornchai, W., Rungrassamee, W., Karoonuthaisiri, N., Jarayabhand, P., Klinbunga, S., Söderhäll, K., Jiravanichpaisal, P., 2010. Expression of immune-related genes in the digestive organ of shrimp, *Penaeus monodon*, after an oral infection by *Vibrio harveyi*. Dev. Comp. Immunol. 34 (1), 19–28. https://doi.org/10.1016/j.dci.2009.07.007.
Soonthornchai, W., Chaiyapechara, S., Jarayabhand, P., Söderhäll, K., Jiravanichpaisal, P., 2015. Interaction of *Vibrio spp*. with the inner surface of the digestive tract of *Penaeus monodon*. PLoS One 10 (8), e0135783. https://doi.org/10.1371/journal.pone.0135783.
Stentiford, G.D., Neil, D.M., Peeler, E.J., Shields, J.D., Small, H.J., Flegel, T.W., Vlak, J. M., Jones, B., Morado, F., Moss, S., Lotz, J., Bartholomay, L., Behringer, D.C., Hauton, C., Lightner, D.V., 2012. Disease will limit future food supply from the global crustacean fishery and aquaculture sectors. J. Invertebr. Pathol. 110 (2), 141–157. https://doi.org/10.1016/j.jip.2012.03.013.
Tani, T., Okamoto, K., Fujiwara, M., Katayama, A., Tsuruoka, S., 2019. Metabolomics analysis elucidates unique influences on purine / pyrimidine metabolism by xanthine oxidoreductase inhibitors in a rat model of renal ischemia-reperfusion injury. Mol. Med. 25 (1), 40. https://doi.org/10.1186/s10020-019-0109-y.
Tassanakajon, A., Amparyup, P., Somboonwiwat, K., Supungul, P., 2010. Cationic antimicrobial peptides in penaeid shrimp. Mar. Biotechnol. (NY) 12 (5), 487–505. https://doi.org/10.1007/s10126-010-9288-9.
Tassanakajon, A., Rimphanitchayakit, V., Visetnan, S., Amparyup, P., Somboonwiwat, K., Charoensapsri, W., Tang, S., 2018. Shrimp humoral responses against pathogens: antimicrobial peptides and melanization. Dev. Comp. Immunol. 80, 81–93. https://doi.org/10.1016/j.dci.2017.05.009.
Tzeng, H.-T., Chyuan, I.T., Chen, W.-Y., 2019. Shaping of innate immune response by fatty acid metabolite palmitate. Cells 8 (12), 1633. https://doi.org/10.3390/cells8121633.
Tzuc, J.T., Escalante, D.R., Rojas Herrera, R., Gaxiola Cortés, G., Ortiz, M.L.A., 2014. Microbiota from *Litopenaeus vannamei*: digestive tract microbial community of Pacific white shrimp (*Litopenaeus vannamei*). SpringerPlus 3 (1), 280. https://doi.org/10.1186/2193-1801-3-280.
Uawisetwathana, U., Plaisen, S., Arayamethakorn, S., Jitthiang, P., Rungrassamee, W., 2021. Optimization of metabolite extraction and analytical methods from shrimp intestine for metabolomics profile analysis using LC-HRMS/MS. Metabolomics 17 (1), 8. https://doi.org/10.1007/s11306-020-01768-x.
Uengwetwanit, T., Uawisetwathana, U., Arayamethakorn, S., Khudet, J., Chaiyapechara, S., Karoonuthaisiri, N., Rungrassamee, W., 2020. Multi-omics analysis to examine microbiota, host gene expression and metabolites in the intestine of black tiger shrimp (*Penaeus monodon*) with different growth performance. PeerJ 8, e9646. https://doi.org/10.7717/peerj.9646.
Uengwetwanit, T., Pootakham, W., Nookaew, I., Sonthirod, C., Angthong, P., Sittikankaew, K., Rungrassamee, W., Arayamethakorn, S., Wongsurawat, T., Jenjaroenpun, P., Sangsrakru, D., Leelatanawit, R., Khudet, J., Koehorst, J.J., Schaap, P.J., Martins Dos Santos, V., Tangy, F., Karoonuthaisiri, N., 2021. A chromosome-level assembly of the black tiger shrimp (*Penaeus monodon*) genome facilitates the identification of growth-associated genes. Mol. Ecol. Resour. 21 (5), 1620–1640. https://doi.org/10.1111/1755-0998.13357.
Underhill, D.M., Ozinsky, A., 2002. Phagocytosis of microbes: complexity in action. Annu. Rev. Immunol. 20 (1), 825–852. https://doi.org/10.1146/annurev.immunol.20.103001.114744.
Valanne, S., Wang, J.H., Rämet, M., 2011. The *Drosophila* Toll signaling pathway. J. Immunol. 186 (2), 649–656. https://doi.org/10.4049/jimmunol.1002302.
Visetnan, S., Supungul, P., Hirono, I., Tassanakajon, A., Rimphanitchayakit, V., 2015. Activation of *Pm*Relish from *Penaeus monodon* by yellow head virus. Fish. Shellfish. Immunol. 42 (2), 335–344. https://doi.org/10.1016/j.fsi.2014.11.015.
Wang, J.-P., Liu, B., Liu, G.-H., Chen, D.-J., Ge, C.-B., Chen, Z., Che, J.-M., 2015. Genome sequence of *Brevibacillus reuszeri* NRRL NRS-1206T, an l-N-carbamoylase-producing *Bacillus*-like bacterium. Genom. Announc. 3 (5) https://doi.org/10.1128/genomeA.01063-15 e01063–01015.
Wang, H.-L., Wang, C., Tang, Y., Sun, B., Huang, J., Song, X., 2018. *Pseudoalteromonas* probiotics as potential biocontrol agents improve the survival of *Penaeus vannamei* challenged with acute hepatopancreatic necrosis disease (AHPND)-causing *Vibrio parahaemolyticus*. Aquaculture 494. https://doi.org/10.1016/j.aquaculture.2018.05.020.
Wang, F., Li, S., Xiang, J., Li, F., 2019a. Transcriptome analysis reveals the activation of neuroendocrine-immune system in shrimp hemocytes at the early stage of WSSV infection. BMC Genomics 20 (1), 247. https://doi.org/10.1186/s12864-019-5614-4.
Wang, Q., Wang, K., Wu, W., Giannoulatou, E., Ho, J.W.K., Li, L., 2019b. Host and microbiome multi-omics integration: applications and methodologies. Biophys. Rev. 11 (1), 55–65. https://doi.org/10.1007/s12551-018-0491-7.
Wang, H., Huang, J., Wang, P., Li, T., 2020. Insights into the microbiota of larval and postlarval Pacific white shrimp (*Penaeus vannamei*) along early developmental stages: a case in pond level. Mol. Gen. Genomics. 295 (6), 1517–1528. https://doi.org/10.1007/s00438-020-01717-2.
Wei, T., Simko, V., 2021. R package 'corrplot': visualization of a correlation matrix. (Version 0.92). github.com/taiyun/corrplot.
Wongpanya, R., Sengprasert, P., Amparyup, P., Tassanakajon, A., 2016. A novel C-type lectin in the black tiger shrimp *Penaeus monodon* functions as a pattern recognition receptor by binding and causing bacterial agglutination. Fish. Shellfish. Immunol. 60 https://doi.org/10.1016/j.fsi.2016.11.042.
Wu, X., Xia, Y., He, F., Zhu, C., Ren, W., 2021. Intestinal mycobiota in health and diseases: from a disrupted equilibrium to clinical opportunities. Microbiome 9 (1), 60. https://doi.org/10.1186/s40168-021-01024-x.
Xiong, J.B., Nie, L., Chen, J., 2019. Current understanding on the roles of gut microbiota in fish disease and immunity. Zool. Res. 40 (2), 70–76. https://doi.org/10.24272/j.issn.2095-8137.2018.069.

Yin, J., Ren, W., Huang, X., Deng, J., Li, T., Yin, Y., 2018. Potential mechanisms connecting purine metabolism and cancer therapy. Front. Immunol. 9 https://doi.org/10.3389/fimmu.2018.01697.

Younes, S., Al-Sulaiti, A., Nasser, E.A.A., Najjar, H., Kamareddine, L., 2020. Drosophila as a model organism in host–pathogen interaction studies. Front. Cell. Infect. Microbiol. 10 https://doi.org/10.3389/fcimb.2020.00214.

Yu, W., Wu, J.H., Zhang, J., Yang, W., Chen, J., Xiong, J., 2018. A meta-analysis reveals universal gut bacterial signatures for diagnosing the incidence of shrimp disease. FEMS Microbiol. Ecol. 94 (10) https://doi.org/10.1093/femsec/fiy147.

Yuan, K., Yuan, F.-H., Weng, S.-P., He, J.-G., Chen, Y.-H., 2017. Identification and functional characterization of a novel Spätzle gene in *Litopenaeus vannamei*. Dev. Comp. Immunol. 68, 46–57. https://doi.org/10.1016/j.dci.2016.11.016.

Zhang, S., Sun, X., 2022. Core gut microbiota of shrimp function as a regulator to maintain immune homeostasis in response to WSSV infection. Microbiol. Spectr. 10 (2), e0246521 https://doi.org/10.1128/spectrum.02465-21.

Zhang, M.L., Shan, C., Tan, F., Limbu, S.M., Chen, L., Du, Z.Y., 2020a. Gnotobiotic models: powerful tools for deeply understanding intestinal microbiota-host interactions in aquaculture. Aquaculture 517, 734800. https://doi.org/10.1016/j.aquaculture.2019.734800.

Zhang, X.-H., He, X., Austin, B., 2020b. *Vibrio harveyi*: a serious pathogen of fish and invertebrates in mariculture. Mar. Life Sci. Technol. 1-15 https://doi.org/10.1007/s42995-020-00037-z.

Zhang, X., Sun, J., Han, Z., Chen, F., Lv, A., Hu, X., Sun, X., Qi, H., Guo, Y., 2021a. *Vibrio parahaemolyticus* alters the community composition and function of intestinal microbiota in Pacific white shrimp, *Penaeus vannamei*. Aquaculture 544, 737061. https://doi.org/10.1016/j.aquaculture.2021.737061.

Zhang, X., Yuan, J., Li, F., Xiang, J., 2021b. Chitin synthesis and degradation in crustaceans: a genomic view and application. Mar. Drug 19 (3). https://doi.org/10.3390/md19030153.

Zhang, Z., Aweya, J.J., Yao, D., Zheng, Z., Tran, N.T., Li, S., Zhang, Y., 2021c. Ubiquitination as an important host-immune response strategy in penaeid shrimp: inferences from other species. Front. Immunol. 12, 697397. https://doi.org/10.3389/fimmu.2021.697397.

Zuo, H., Gao, J., Yuan, J., Deng, H., Yang, L., Weng, S., He, J., Xu, X., 2017. Fatty acid synthase plays a positive role in shrimp immune responses against *Vibrio parahaemolyticus* infection. Fish. Shellfish. Immunol. 60, 282–288. https://doi.org/10.1016/j.fsi.2016.11.054.